Hidden conflict in pollination and its implications for diversification

Foen Peng

A dissertation
submitted in partial fulfillment of
the requirements for the degree of

Doctor of Philosophy

University of Washington
2018

Reading Committee:
H.D. Bradshaw, Jr.
Thomas L. Daniel
Benjamin Kerr

Program Authorized to Offer Degree:
Biology

University of Washington

Abstract

Hidden conflict in pollination and its implications for diversification

Foen Peng

Chairs of the Supervisory Committee:

H.D. Bradshaw, Jr.

Thomas L. Daniel

Department of Biology

Pollinator-driven selection plays an important role in flowering plant diversification. Different pollinator guilds (*e.g.,* butterfly, hummingbird, bat) have different preferences for and performance on flowers, which in turn generates selective forces on plant evolution. In response to these selective forces, plants often evolve a suite of floral traits called a "pollination syndrome" to adapt to their most efficient pollinator guild. Therefore, floral traits which affect both the plant's and the pollinator's fitness are the key to understanding how plant-pollinator interaction influences diversification.

I first examined the genetic basis of floral scent evolution in *Mimulus*, discovering that parallel loss-of-function in the *OCIMENE SYNTHASE* gene, whose protein product synthesizes a floral scent important for bumblebee attraction, can be explained by divergent selection by different pollinator guilds in different *Mimulus* taxa. This result adds support to the notion that pollinator-driven selection has a large impact on floral trait evolution and promotes plant speciation.

Next, I employed a morphospace analysis approach to examine the fitness consequences of corolla shape variation on both plant and pollinator, through a combination of 3D-

printing, electronic sensing, and machine vision. I found that corolla curvature variation can generate a conflict of evolutionary interest between plants and their hawkmoth pollinators as a consequence of the disparate requirements from pollination: efficient pollen transfer for the plant *vs.* efficient resource exploitation by the pollinator.

Finally, I compared the fitness landscape of two different pollinator guilds – hummingbirds and hawkmoths – on a common set of flower shapes with variation in petal curvature and reflexing. I found that a conflict of interest also exists in hummingbird pollination.

Taken together, pollinator specificity is an important ecological factor that influences flowering plant diversification, and the finding of a conflict of interest between plant and pollinator suggests that the framework used to understand diversification driven by antagonistic species interactions can be extended to understanding diversification promoted by seemingly cooperative plant-pollinator interactions.

Table of Contents

Acknowledgment

It has been a tremendously rewarding experience for me to study for my PhD at the University of Washington. I am deeply grateful to the people, the department, the university, and the city.

My co-advisors Toby and Tom give me strong support during my PhD. They are both my academic mentors and role models for life. Their enthusiasm for biological research, positive attitude towards life, and great sense of humor are contagious, which helped me form my own research goals and life goals. The other two members of my committee, Ben and Harmit, gave my favorite courses in graduate school. They were always supportive, inspiring, and fun to talk with.

I'd also like to thank my cohort and friends in Seattle and Portland. My years in the Pacific Northwest have been so much fun because of their company.

Lastly, I want to thank my wife Wei and my family in China. They have always trusted my decisions and given me firm support.

Introduction

Flowering plants (angiosperms) are by far the most speciose group in the plant kingdom and are the dominant organisms (by biomass) in most terrestrial ecosystems. One of the most noteworthy phenomena in flowering plants is the bewildering diversity of floral traits, such as color, patterning, scent, shape, symmetry, and orientation. This variation in floral traits is tightly correlated with plant speciation mediated by animal pollination.

A longstanding hypothesis explaining flowering plant diversification is that different pollinator guilds, such as bees, moths, birds, and bats, differ in their preference for and performance on different flower morphs because of the pollinators's inherent differences in morphology, physiology, and behavior. Pollinator-mediated selection drives corresponding adaptations in floral traits, and the subsequent assortative mating *via* specialized pollinator visits can generate prezygotic reproductive isolation among plant populations, which ultimately leads to flowering plant speciation. Because of the mutually beneficial, specialized interaction between a plant and its pollinator, plant populations should evolve a suite of floral traits (*i.e.,* pollination syndrome) that maximize both the fitness of the plant itself and the animal pollinator. Geographical and temporal variation in pollinator communities could affect the direction and strength of selection that the pollinator exerts on the plant. Thus, plant diversification can be accelerated *via* pollinator-shift from one pollinator guild to another.

One theoretical difficulty with this hypothesis is that once a plant species forms a stable mutualistic pollination relationship with its most efficient pollinator, further diversification is hindered by stabilizing selection on the mutualistic partnership, because any deviation from the norm will likely decrease both partners' fitness. For example, mismatch between the timing of plant flowering and the timing of the pollinating insect's eclosion decreases both the plant's and the insect's fitness. Consequently, both partners are trapped on their adaptive peaks and cannot promote further diversification.

In this thesis, I assume that natural selection acts on each partner of the pollination interaction, instead of on the partnership as a unit. So each partner maximizes its own fitness, which may or may not be aligned with the other partner's fitness. Any fitness misalignment can generate conflict between the two partners, which will break the hypothetical equilibrium of the stable relationship and potentially promote diversification.

In Chapter 1, I empirically examine the evolution of pollination syndromes in the *Erythranthe* section of the wildflower genus *Mimulus*. I find that the *Mimulus* taxa closely related to the bumbleblee specialist,*Mimulus lewisii*, but which are not themselves pollinated by bumblebees, all have lost ocimine production, a floral trait that is important for bumblebee attraction. This phenomenon is caused by parallel, independent loss-of-function mutations in the *OCIMENE SYNTHASE* gene, which encodes the enzyme responsible for ocimene production. This parallel loss-of-function finding suggests that pollinator-mediated selection is likely to promote floral trait differentiation.

In Chapter 2, I describe a novel approach to detecting the potential conflict of interest between plant and pollinator. By exploring the fitness landscape of floral trait variation (morphospace) using a combination of 3D printing, automated sensing, and machine vision, I found that hawkmoth pollinators and plants have a strong conflict of interest in the evolution of corolla curvature.

In Chapter 3, I compared the fitness landscapes of two different pollinator guilds, hummingbirds and hawkmoths, to explore the potential avenue for speciation by pollinator shift. I found strong conflict between the plant and the hummingbird pollinator in the evolution of corolla curvature. Variation along the two floral shape axes tested in this study, corolla curvature and petal reflexing, cannot distinguish the two pollinators.

In Chapter 4, I review the literature on species interactions and diversification, and suggest that conflict in cooperative interactions can act in a similar manner as antagonistic interactions in promoting diversification.

In summary, I developed a novel approach to experimentally quantify the fitness of both parties in the plant and pollinator interaction, explored flower morphospace along several axes, and found conflicts between plant and pollinators. The methodological innovation adds a new toolkit for the traditional pollination studies, and the conflict of interest finding advances our theoretical understanding of plant diversification.

Chapter 1

Less is more: independent loss-of-function *OCIMENE SYNTHASE* alleles parallel pollination syndrome diversification in monkeyflowers (*Mimulus*)

Short title: Loss-of-function mutations parallel *Mimulus* diversification

Foen Peng[2], Kelsey J. R. P. Byers[2, 3], Harvey D. Bradshaw, Jr.[2,4]

[1] Manuscript received _____; revision accepted _____.

[2] Department of Biology, University of Washington, Seattle, WA 98195, USA;

[3] Department of Zoology, University of Cambridge, Cambridge, England, UK

[4] Author for correspondence, email toby@uw.edu

Abstract

- *Premise of the study:* Pollinator-mediated selection on flower phenotypes (*e.g.*, shape, color, scent) is key to understanding the adaptive radiation of angiosperms, many of which have evolved specialized relationships with a particular guild of animal pollinators (*e.g.*, birds, bats, moths, bees). *E*-β-ocimene, a monoterpene produced by OCIMENE SYNTHASE (OS), is a flower scent important in attracting *Mimulus lewisii*'s bumblebee pollinators. The taxa closely related to *M. lewisii* have evolved several different pollination syndromes, including hummingbird pollination and self pollination (autogamy). We are interested in how floral scent variation contributed to species diversification in this clade.

- *Methods:* We analyzed variation in *E*-β-ocimene emission within this *Mimulus* clade and explored its molecular basis through a combination of DNA sequencing, reverse transcriptase PCR, and enzyme functional analysis *in vitro*.

- *Key results:* We found that all the taxa, other than *M. lewisii*, emitted no *E*-β-ocimene from flowers. But the molecular basis underlying loss of *E*-β-ocimene emission is unique in each taxon, including deletion, missense, or frameshift mutations in the *OS* gene, and potential post-transcriptional downregulation.

- *Conclusions:* The molecular evidence suggests that parallel loss-of-function in *OS* is the best explanation for the observed pattern of *E*-β-ocimene emission, likely as the result of natural selection.

Key words: Floral scent; loss-of-function mutation; *Mimulus*; parallel evolution; pollination

INTRODUCTION

Flower scent is one of the floral traits that strongly influences animal behavior, and is an important factor in pollinator discrimination. Pollinators use the volatiles emitted by flowers as long-distance signals, landing cues, or feeding cues (Raguso, 2008). Plants pollinated by similar groups of pollinators tend to have similar scent profiles (Dobson 2006; Riffell *et al.,* 2013; Schiestl and Johnson, 2013). Changes in floral scent can drive pollinator shifts (Vereecken *et al.,* 2009; Shuttleworth and Johnson, 2010; Klahre *et al.*, 2011), which contribute to plant reproductive isolation, and lead to adaptive divergence. Despite the important ecological role of floral scent in influencing plant pollination, little is known about how the genes controlling floral scent emission contribute to plant evolution (Schiestl and Johnson, 2013). The genetic basis of floral scent profiles has been characterized in only a few cases (*e.g., Clarkia* (Dudareva *et al.,* 1996), *Antirrhinum* (Dudareva *et al.,* 2003), *Petunia* (Klahre *et al.*, 2011), and *Mimulus* (Byers *et al.,* 2014b)). The genetic basis of repeated evolution in floral scent has not been reported.

The sister species pair from *Mimulus* section *Erythranthe*, *Mimulus lewisii* (bumblebee-pollinated) and *Mimulus cardinalis* (hummingbird-pollinated), is a classical model system for pollination ecology and evolutionary genetics research (Hiesey *et al.,* 1971; Schemske and Bradshaw, 1999; Bradshaw and Schemske, 2003). Byers *et al.* (2014a) characterized distinct scent profiles between flowers of the two species: bumblebee specialist *M. lewisii* (southern race) has a high emission rate of three terpenes: D-limonene, β-myrcene, and *E*-β-ocimene, which evoke a strong neural response in bumblebees, while hummingbird specialist *M. cardinalis* emits these compounds at less than 1% the rate of *M. lewisii*. The difference in *E*-β-ocimene emission between *M. lewisii* and *M. cardinalis* flowers is due to allelic variation in the *OCIMENE SYNTHASE* (*OS*) gene (Byers *et al.,* 2014b). When *E*-β-ocimene emission is eliminated in transgenic southern *M. lewisii* plants by targeting *OS* with RNAi, visitation by bumblebees is significantly decreased (Byers *et al.,* 2014b). Therefore, *E*-β-ocimene is a key component in the floral scent bouquet of southern *M. lewisii*, and *OS* is a key gene that influences pollination syndrome evolution.

M. lewisii includes two well-supported sister races: a southern race distributed in the Sierra Nevada, and a northern race in the Cascades and Rocky Mountains. Although they differ in corolla color and size and have also evolved partial postzygotic isolation, both races are primarily pollinated by bumblebees (Hiesey *et al.,* 1971; Beardsley *et al.,* 2003). Ancestral state reconstruction analysis based on a highly supported species tree suggests that the common ancestor of *Erythranthe* is also insect-pollinated (Beardsley *et al.,* 2003) (Fig 1). *M. bicolor*, the outgroup of *Erythranthe* in this phylogeny, is mostly pollinated by small-bodied (halictid) bees (Grossenbacher and Stanton, 2014). Yet within the *Erythranthe*, only *M. lewisii* is insect-pollinated. *M. cardinalis* is a hummingbird specialist, *M. parishii* is self-pollinated, and the subclade containing *M. verbenaceus* has independently evolved the hummingbird pollination syndrome (Beardsley *et al.,* 2003) (Fig. 1). This interesting pattern of pollination syndrome evolution in *Erythranthe* suggested that pollinator shift might have played an important role in the speciation and diversification process.

In the present study, we test the hypothesis that the flowers of related taxa, if not bumblebee specialists, would not produce *E*-β-ocimene. We also investigate the molecular mechanisms underpinning the variation in *E*-β-ocimene emission phenotypes.

MATERIALS AND METHODS

Plant materials and growth conditions

Seeds of each taxon were collected from several locations in the USA (Table S1) for *M. lewisii* southern race*, M. lewisii* northern race*, M. cardinalis, M. parishii, M. verbenaceus*, and *M. bicolor*. Plants (Table S1) were grown in identical controlled conditions (Yuan *et al.,* 2013) in the New Botany Greenhouse of the University of Washington, Seattle, WA, USA, until flowering.

Flower volatiles collection and analysis

Floral volatiles of every plant were collected for 24 hours from the headspace of two newly-opened flowers at the same node, and analyzed by gas chromatography-mass spectrometry (GCMS). Protocols and analysis are described in detail in Byers *et al.*

(2014a). The *in vivo E*-β-ocimene emission variation was analyzed by pairwise Wilcoxon rank sum test, using R version 3.0.2.

OCIMENE SYNTHASE sequencing

To obtain the orthologous *OS* sequences from all taxa*,* the southern *M. lewisii OS* coding sequence (GenBank accession number: KF857262) was used to BLAST (Altschul *et al.,* 1990) against the genome of *M. verbenaceus* and the flower petal transcriptome of *M. bicolor,* which were previously sequenced following the protocols described in Yuan *et al.* (2013) and Yuan *et al.* (2014). For *M. lewisii* southern and northern races, *M. cardinalis*, and *M. parishii*, full length *OS* coding sequences were also amplified from floral cDNA libraries by PCR. The primer pair used for PCR was OS_TOPO_F1 caccATGGACGTAGAATCGGCTAACCAC and OS_TOPO_R1 TTAATTAGGGCAAGGTAGAGGAAGA. Samples were amplified with Phusion High-Fidelity DNA Polymerase (New England Biolabs) under the following conditions: $95\,^{\circ}\text{C}$ for 3 min, followed by 35 cycles of $95\,^{\circ}\text{C}$ for 15 s, $53\,^{\circ}\text{C}$ for 30 s, and $72\,^{\circ}\text{C}$ for 1 min. The PCR products were sequenced in both directions by Sanger sequencing (GENEWIZ, Seattle).

RNA extraction and Reverse Transcriptase PCR (RT-PCR)

Total RNA of *M. lewisii* southern and northern races, *M. cardinalis*, and *M. parishii* was isolated from the petals of fully open flowers, which have the highest level of *OS* expression among all flower development stages in both *M. lewisii* and *M. cardinalis* (Byers *et al.,* 2014b). cDNA was prepared from 1μg of DNAase-treated total RNA, using the SuperScript III First-Strand Synthesis System (Invitrogen). RT-PCR was performed with the cDNA library for each taxon, using the *Mimulus* ortholog of *Ubiquitin-Conjugating Enzyme* (*UBC)* fragment as a control for expression levels (Yuan *et al.,* 2013). Gene-specific primers for RT-PCR were designed from the *OS* coding sequence alignment (OS-1F: CAGTGGGAGACGAACAGCCAATTAC; OS-1R: TGATAGCCGTACTGCCTCATGATC). Samples were amplified under the following conditions: $95\,^{\circ}\text{C}$ for 3 min, followed by 35 cycles of $95\,^{\circ}\text{C}$ for 15 s, $46\,^{\circ}\text{C}$ for 30 s, and $72\,^{\circ}\text{C}$ for 30 s. There were no visible bands after 31 cycles, so we analyzed PCR products

after 35 cycles.

In vitro assay for OCIMENE SYNTHASE activity

For *M. lewisii* southern and northern races, *M. cardinalis*, and *M. parishii,* the coding sequence of *OS* was cloned into pET100/D-TOPO vector and transformed into *E. coli* strain BL21 following the manufacturer's instructions (Invitrogen). Enzyme overexpression and terpene synthase activity measurement followed the protocol of Fäldt *et al*. (2003), and *E*-β-ocimene production was assayed by GCMS as previously described (Byers *et al*., 2014a,b).

RESULTS

In vivo emission of E-β-ocimene

In vivo (flower) emission of *E*-β-ocimene is very low and not significantly different among *M. cardinalis* (0.028 ± 0.013 ng/hr), *M, parishii* (0.008 ± 0.002 ng/hr), *M. verbenaceus* (0.023 ± 0.012 ng/hr)*,* and *M. bicolor* (0.002 ± 0.001 ng/hr) (Wilcoxon rank sum test, $p > 0.5$, Table S2), and all of them emit much less *E*-β-ocimene than *M. lewisii* southern and northern races ($p < 0.05$, Table S2). Southern *M. lewisii* flowers emit significantly more (7.799 ± 1.373 ng/hr) *E*-β-ocimene than northern *M. lewisii* flowers (1.116 ± 0.206 ng/hr) ($p = 9.5e-08$) (Fig. 2a).

OCIMENE SYNTHASE sequence analysis

The reference *OS* coding sequence in southern *M. lewisii* (KF857262) has seven exons. BLAST search against the genomes of southern *M. lewisii*, *M. cardinalis*, and *M. verbenaceus* suggests that *OS* existed as a single copy. The second best hit is a short pseudogenized fragment without recognizable continuous reading frames. The orthologous *OS* coding sequences of northern *M. lewisii* (KX902512), *M. cardinalis* (KF857263), and *M. parishii* (KX902509) have some small indels and nonsynonymous mutations (26, 18, and 23 amino acid differences, respectively, referencing to southern *M. lewisii*) (Fig. 3). *M. verbenaceus OS* (KX902510) contains a large deletion from the third exon to the last exon. The *OS* ortholog in *M. bicolor* (KX902511) has a 2bp insertion in the second exon, producing a frameshift mutation and premature termination

(Fig. 3 and Fig. S1). We excluded *M. verbenaceus* and *M. bicolor* from subsequent expression and enzyme activity analysis because of the obvious loss-of-function mutations that they carry.

OCIMENE SYNTHASE expression analysis

The RT-PCR results show that there are no *OS* steady-state expression differences between southern *M. lewisii*, northern *M. lewisii*, *M. cardinalis*, and *M. parishii* at the open flower stage (Fig. 2b).

OCIMENE SYNTHASE enzyme activity analysis *in vitro*

Except for *M. parishii*, the relative *E*-β-ocimene production pattern *in vitro* by OS enzymes from southern *M. lewisii*, northern *M. lewisii,* and *M. cardinalis* tracks the *E*-β-ocimene emission pattern by flowers *in vivo* (Fig. 2a). The *E*-β-ocimene production relative to southern *M. lewisii in vitro* are: northern *M. lewisii* 14.44%, *M. cardinalis* 0.74%, *M. parishii* 99.96%. Surprisingly, given the very low *E*-β-ocimene emission *in vivo*, *M. parishii* has a fully functional OS enzyme *in vitro*.

DISCUSSION

M. lewisii, the bumblebee specialist, is the only species in *Mimulus* section *Erythranthe* that emits *E*-β-ocimene. The different *OS* mutations carried by *M. cardinalis* (missense) and *M. verbenaceus* (deletion) indicate that these loss-of-function *OS* alleles are independently derived, rather than being inherited from a common ancestor. We conclude that the most likely explanation for the observed pattern is parallel evolution of loss-of-function alleles.

The out-group species *M. bicolor* has also independently lost functional *OS*, which suggests that *E*-β-ocimene may not be attractive to small-bodied (halictid) bees.

Pre-existing biases on floral signals of pollinators can exert strong selection pressures on floral phenotype (Schiestl and Johnson, 2013). *E*-β-ocimene, which evokes a strong neural response from bumblebees, is a key volatile in *M. lewisii*'s scent bouquet (Byers *et*

11

al., 2014a). It acts in concert with other volatiles and other flower traits (*e.g.,* carotenoid-pigmented nectar guide, wide corolla opening) to form the bumblebee pollination syndrome in *M. lewisii*. While related species evolved new pollination syndromes (*i.e.,* hummingbird pollination), the *E*-β-ocimene emission trait was no longer advantageous. As a result, loss-of-function mutations in *OS* could accumulate and be fixed; in principle, either by genetic drift or by natural selection. Natural selection is the more likely explanation, because mismatched flower visitors will cause pollen loss, thus reducing male fitness (Thomson, 2003). For example, mechanical "anti-bee" adaptation in *Penstemon* is important in transitions from the bee pollination syndrome to the hummingbird pollination syndrome (Castellanos *et al.,* 2004)

Northern *M. lewisii* emits *E*-β-ocimene, though at a rate almost 7 times lower than southern *M. lewisii*. Byers *et al.* (2014b) used RNAi to knock down *OS* expression in southern *M. lewisii* flowers from 5.56 ng/hr to 0.05ng/hr, which caused a 6% decrease in bumblebee visitation. The reduced level of *E*-β-ocimene in northern *M. lewisii* flowers does not impair bumblebees' ability to recognize and visit northern *M. lewisii* flowers, which suggests that either the *E*-β-ocimene production rate in northern *M. lewisii* is sufficient for bumblebees to visit the flower, or that other floral traits in northern *M. lewisii*, such as a more intense corolla color and larger size, might compensate for the reduced *E*-β-ocimene production in pollinator attraction.

M. parishii is self-pollinated. Surprisingly, although *M. parishii* flowers do not emit *E*-β-ocimene, the *OS* gene is highly expressed in flower petals (Fig. 2b) and the *OS* coding sequence is fully functional when expressed *in vitro* (Fig. 2a). We speculate that a post-transcriptional regulatory mechanism might be responsible for the loss of *E*-β-ocimene emission in *M. parishii* flowers. Evidence suggests that terpene synthetic pathways can be regulated at the post-transcriptional or post-translational levels (Tholl, 2006; Patra *et al.*, 2013)

Application of the parsimony principle to the pattern of *E*-β-ocimene emission shown in Fig. 1 would lead us to conclude that the *M. lewisii* phenotype is the result of a gain-of-

function mutation, but our molecular analysis suggests that parallel independent loss-of-function in the other taxa is much more likely. Parallel loss-of-function has been identified in many systems as the underlying molecular mechanisms for repeated phenotypic evolution. For example, the color transition from blue to red in several species of *Penstemon* involves parallel loss-of-function mutations in the gene encoding flavonoid 3′,5′-hydroxylase (F3′5′H) (Wessinger and Rausher, 2015). In *Ipomoea*, the same repeated color transition pattern (blue to red) results from the down-regulation of another enzyme in the same pathway, flavonoid 3′-hydroxylase (F3′H), in two independent cases (Streisfeld and Rausher, 2009). In *Petunia axillaris*, independent pseudogenization of *AN2* (a MYB transcription factor regulating the anthocyanin biosynthetic pathway) in different subspecies contributed to flower color transitions from pigmented to white (Quattrocchio *et al.,* 1999). *FRIGIDA,* a major determinant of flowering time in *Arabidopsis thaliana*, evolved an early-flowering phenotype at least twice from a late-flowering ancestor by independent loss-of-function deletions (Johanson *et al.,* 2000). Independent pelvic spine reduction in sticklebacks from isolated lakes in North America is caused by parallel regulatory region mutations in *Pitx1* causing expression level changes (Chan *et al.,* 2010). Taken together, we suggest that loss-of-function mutations might be a common source of evolutionary innovations in nature. And evolution does not necessarily follow a parsimonious path, so caution should be used in interpretation of character state evolution when the mutations underlying those phenotypes are unknown.

These evolutionary parallelisms not only stress the critical role of natural selection in phenotypic diversification and speciation, but also suggest that evolution has a limited "tool kit." The genes whose different alleles maximize phenotypic output while minimizing pleiotropic effects will be overrepresented in evolutionary trajectories (Stern, 2011). The importance of genes responsible for pollination syndrome transitions identified in model systems could be further verified by comparative studies in non-model organisms.

We have shown that parallel loss-of-function of a scent gene, *OCIMENE SYNTHASE*, corresponds with pollination syndrome diversification in a *Mimulus* clade. The repeated loss of function in the *OS* gene suggests that the loss of ancestral flower traits can be an important, and potentially irreversible, mechanism to facilitate pollination syndrome transition.

Acknowledgments

LITERATURE CITED

Altschul, S.F., W. Gish, W. Miller, E.W. Myers, and D.J. Lipman. 1990. Basic local alignment search tool. *Journal of Molecular Biology* 215:403–410.

Beardsley, P.M., A. Yen, and R.G. Olmstead. 2003. AFLP phylogeny of *Mimulus* section *Erythranthe* and the evolution of hummingbird pollination. *Evolution* 57: 1397–1410.

Bradshaw, H.D., and D.W. Schemske. 2003. Allele substitution at a flower colour locus produces a pollinator shift in monkeyflowers. *Nature* 426:176–178.

Byers, K.J.R.P., H.D. Bradshaw, and J.A. Riffell. 2014a. Three floral volatiles contribute to differential pollinator attraction in monkeyflowers (*Mimulus*). *Journal of Experimental Biology* 217:614–623.

Byers, K.J.R.P., J.P. Vela, F. Peng, J.A. Riffell, and H.D. Bradshaw. 2014b. Floral volatile alleles can contribute to pollinator-mediated reproductive isolation in monkeyflowers (*Mimulus*). *The Plant Journal* 80: 1031–1042.

Castellanos, M. C., P. Wilson, and J. D. Thomson. 2004. 'Anti-bee' and 'pro-bird' changes during the evolution of hummingbird pollination in *Penstemon* flowers. *Journal of evolutionary biology*, 17(4), 876-885.

Chan, Y.F., M.E. Marks, F.C. Jones, G. Villarreal, M.D. Shapiro, S.D. Brady, A.M. Southwick, et al. (2010). Adaptive evolution of pelvic reduction in sticklebacks by recurrent deletion of a *Pitx1* enhancer. *Science* 327: 302–305.

Dobson, H.E. 2006. Relationship between floral fragrance composition and type of pollinator. *Biology of floral scent*. CRC Press, 147-198.

Dudareva, N., L. Cseke, V.M. Blanc, and E. Pichersky. 1996. Evolution of floral scent in *Clarkia*: novel patterns of S-linalool synthase gene expression in the *C. breweri* flower. *The Plant Cell* 8: 1137-1158.

Dudareva, N., D. Martin, C.M. Kish, N. Kolosova, N. Gorenstein, J. Fäldt, B. Miller, and J. Bohlmann. 2003. (*E*)- β-ocimene and myrcene synthase genes of floral scent biosynthesis in snapdragon: function and expression of three terpene synthase genes of a new terpene synthase subfamily. *The Plant Cell* 15: 1227–1241.

Fäldt, J., D. Martin, B. Miller, S. Rawat, and J. Bohlmann. 2003. Traumatic resin defense in Norway spruce (*Picea abies*): Methyl jasmonate-induced terpene synthase gene expression, and cDNA cloning and functional characterization of (+)-3-carene synthase. *Plant Molecular Biology* 51: 119–133.

Grossenbacher, D.L., and M.L. Stanton. 2014. Pollinator-mediated competition influences selection for flower-color displacement in sympatric monkeyflowers. *American Journal of Botany* 101: 1915-1924

Hiesey, W.M., M.A. Nobs, and O. Bjorkman. 1971. Experimental studies on the nature of species: 5. Biosytematics, genetics and physiological ecology of the *Erythranthe* section of *Mimulus*. Washington: DC Carnegie Inst. vi, 213p.(Publ. 628). Illustrations.

Johanson, U., J. West, C. Lister, S. Michaels, R. Amasino, and C. Dean. 2000. Molecular analysis of *FRIGIDA*, a major determinant of natural variation in *Arabidopsis* flowering time. *Science* 290: 344–347.

Klahre, U., A. Gurba, K. Hermann, and M. Saxenhofer. 2011. Pollinator choice in *Petunia* depends on two major genetic loci for floral scent production. *Current Biology* 21: 730-739

Patra, B., C. Schluttenhofer, Y. Wu, S. Pattanaik, and L. Yuan. 2013. Transcriptional regulation of secondary metabolite biosynthesis in plants. *Biochimica et Biophysica Acta (BBA) - Gene Regulatory Mechanisms* 1829: 1236–1247.

Quattrocchio, F., J. Wing, K. van der Woude, E. Souer, N. de Vetten, J. Mol, and R. Koes. 1999. Molecular analysis of the *anthocyanin2* gene of *Petunia* and its role in the evolution of flower color. *The Plant Cell*, 11(8): 1433-1444.

Raguso, R.A. 2008. Wake Up and Smell the Roses: The Ecology and Evolution of Floral Scent. *Annual Review of Ecology, Evolution and Systematics* 39:549–569.

Riffell, J.A., H. Lei, L. Abrell, and J.G. Hildebrand. 2013. Neural Basis of a Pollinator's Buffet: Olfactory Specialization and Learning in *Manduca sexta*. *Science* 339: 200–204.

Schiestl, F.P., and S.D. Johnson. 2013. Pollinator-mediated evolution of floral signals. *Trends in Ecology & Evolution* 28: 307–315.

Schemske, D.W., and H.D. Bradshaw. 1999. Pollinator preference and the evolution of floral traits in monkeyflowers (*Mimulus*). *Proceedings of the National Academy of Sciences, USA* 96: 11910–11915.

Shuttleworth, A., and S.D. Johnson. 2010. The missing stink: sulphur compounds can mediate a shift between fly and wasp pollination systems. *Proceedings of the Royal Society of London, B, Biological Sciences* 277: 20100491–2819.

Stern, D.L. 2011. *Evolution, development, & the predictable genome*. Roberts and Co. Publishers.

Streisfeld, M.A., and M.D. Rausher. 2009. Genetic changes contributing to the parallel evolution of red floral pigmentation among *Ipomoea* species. *New Phytologist* 183: 751–763.

Tholl, D. 2006. Terpene synthases and the regulation, diversity and biological roles of terpene metabolism. *Current Opinion in Plant Biology* 9: 297–304.

Thomson, J. 2003. When Is It Mutualism? *American Naturalist* 162:S1–S9.

Vereecken, N.J., S. Cozzolino, and F.P. Schiestl. 2010. Hybrid floral scent novelty drives pollinator shift in sexually deceptive orchids. *BMC Evolutionary Biology* 10: 103.

Wessinger, C.A., and M.D. Rausher. 2015. Ecological transition predictably associated with gene degeneration. *Molecular Biology and Evolution* 32: 347–354.

Yuan, Y.W., J.M. Sagawa, L. Frost, J.P. Vela, and H.D. Bradshaw. 2014. Transcriptional control of floral anthocyanin pigmentation in monkeyflowers (*Mimulus*). *New Phytologist* 204: 1013-1027

Yuan, Y.W., J.M. Sagawa, R.C. Young, B.J. Christensen, and H.D. Bradshaw. 2013. Genetic dissection of a major anthocyanin QTL contributing to pollinator-mediated reproductive isolation between sister species of *Mimulus*. *Genetics* 194: 255–263.
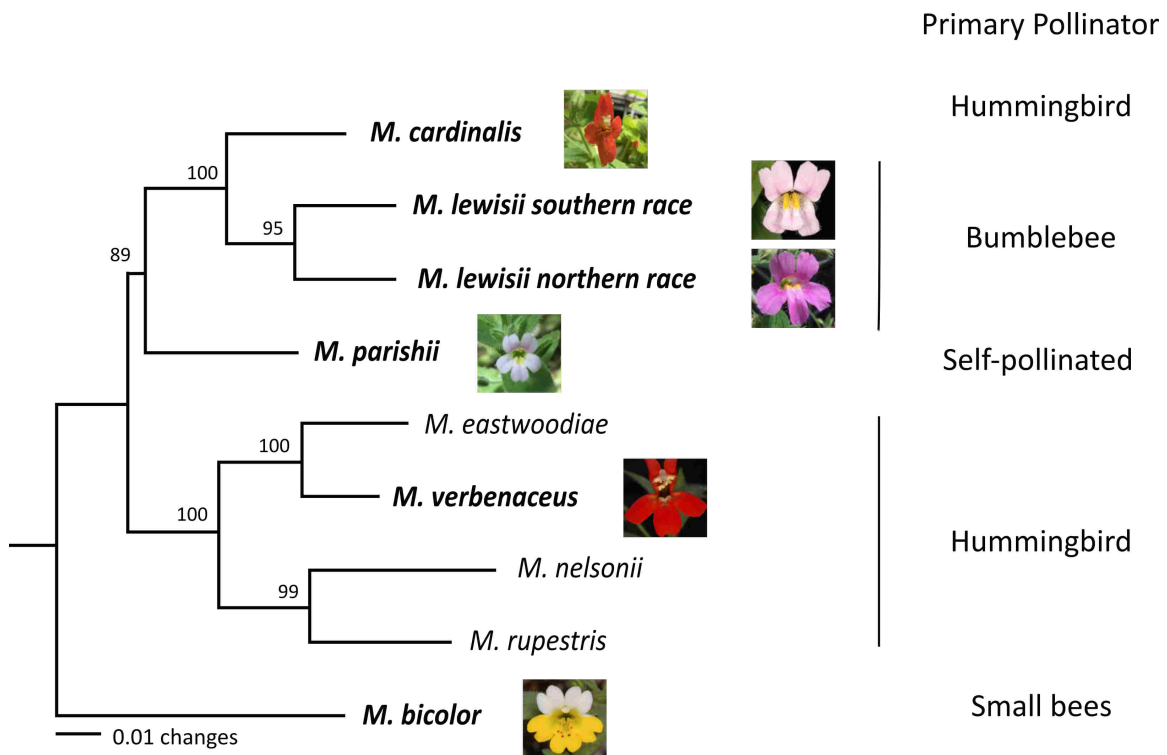
Fig. 1. A phylogeny of the *Mimulus* species in this study. This neighbor-joining tree was constructed by Beardsley *et al.,* 2003 using AFLP fragments. The numbers indicates bootstrap support values for subtending nodes. The names of the species in this study are in bold. The pollinator guild is indicated on the right side. Photo credits: Yaowu Yuan
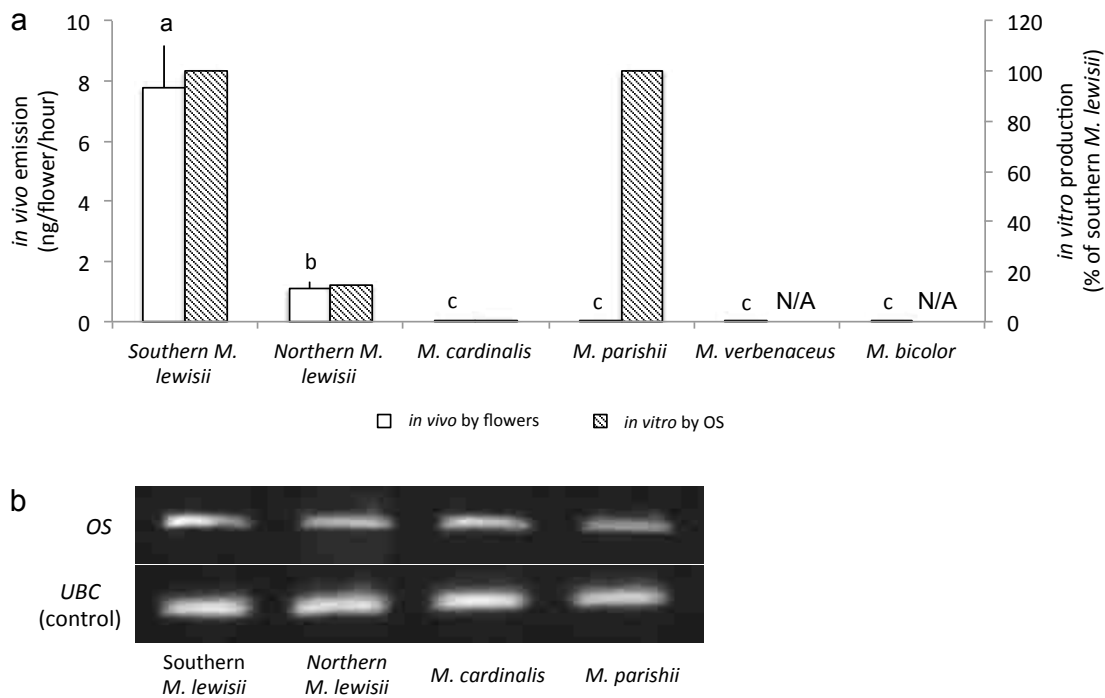
Fig. 2. (a) E-β-ocimene production by flowers *in vivo* (error bars represent standard error) and relative E-β-ocimene production from the OS enzyme *in vitro* (southern *M. lewisii* as 100%). (b) *OS* mRNA levels in the open flower stage by RT-PCR, relative to the *UBC* control. *M. verbenaceus* and *M. bicolor* were not included in the enzyme activity and expression analysis because they carry obvious loss-of-function mutations.
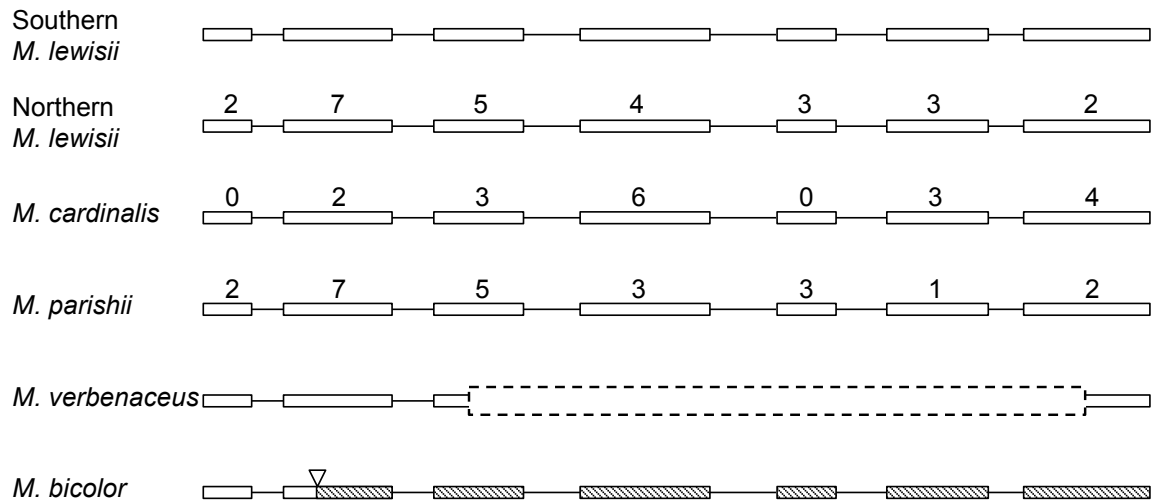
Fig. 3. *OCIMENE SYNTHASE* sequence comparison. Open boxes indicate exons and solid lines indicate introns. The lengths of boxes and lines are proportional to the lengths of DNA sequences. The number of amino acid differences between southern *M. lewisii* and other taxa are indicated above each box. *M. verbenaceus* has a large deletion and *M. bicolor* has a frameshift mutation.

Chapter 2

Conflict of evolutionary interests between plants and pollinators revealed through functional exploration of flower morphospace

Foen Peng[†], Eric O. Campos[†], Joseph Garret Sullivan, Nathan Berry, Bo Bin Song,

Thomas L. Daniel, and H. D. Bradshaw, Jr. *

Department of Biology, University of Washington, Seattle, Washington 98195, USA

[†] Both authors contributed equally to this work.

* Correspondence: toby@uw.edu

Abstract

The explosive evolutionary diversification of flowering plants traditionally is attributed to the coevolution of plants and their animal pollinators. Plant-pollinator interactions are held as classical examples of mutualisms – beneficial to both parties – in spite of the fact that most other cases of rapid coevolution are the result of conflicts of interest (*e.g.*, predator-prey, host-parasite, sexual conflict, competition for resources). Could the co-diversification of plants and their pollinators be driven by conflict rather than by mutualism? To address this question, we employed the theoretical morphospace paradigm using a combination of 3D printing, electronic sensing, and machine vision technologies to determine the influence of two flower morphological features (corolla curvature and nectary diameter) on the fitness of both parties: the artificial flower and its hawkmoth pollinator. We found that the two parties have almost opposite interests in corolla curvature evolution, with non-overlapping fitness peaks in flower morphospace, suggesting that the evolutionary radiation of flowering plants and their pollinators could be the result of conflict instead of mutualism.

Keywords

Introduction

Flowering plants (angiosperms) are the most diverse lineage in the plant kingdom. Their initial major diversification happened in the early Cretaceous (about 130 - 190 Mya), which was accompanied by the co-radiation of pollinating insects [1,2]. This rapid co-diversification process has been attributed to mutual adaptations for biotic pollination. At least a quarter of divergence events in flowering plants are associated with pollinator shifts [3].

Traditionally, plant-pollinator interactions are considered to be classical examples of mutualism – increasing the fitness of both parties [4]. Pollinators provide plants with pollen transport services leading directly to offspring production, while plants provide pollinators with many types of rewards, such as energy-rich nectar [5], shelter [6], or thermoregulation [7], that enhance the survival, growth, and reproduction of the pollinators.

However, most examples of rapid coevolutionary diversification are the result of conflicts of interest rather than mutualisms [8]. For example, food competition drives stickleback populations to diverge into a "limnetic" species and a "benthic" species [9]. Similarly, the arms race between plant (prey) chemical defenses and caterpillar (predator) counter-defenses promotes diversification in both groups [10]. Host-parasite [11] and male-female conflicts [12] likewise increase the rates of coevolutionary diversification.

In contrast, mutualistic coevolution assumes that each party maximizes its own fitness only when its phenotype matches the needs of its partner. These matching phenotypes should be maintained by stabilizing selection, thus hindering diversification [8]. The orthodox view of the plant-pollinator relationship as a mutualism cannot easily explain the rapid diversification of angiosperms and insects. Therefore, we test the counterintuitive hypothesis that there is a conflict of interest between plants and their pollinators.

Flower morphology is key to understanding plant-pollinator interactions, which is exemplified by Darwin's famous prediction of the existence of a hawkmoth species with a long proboscis to match the extraordinarily long nectar spur of a Malagasy orchid [13]. Previous studies have shown that many flower morphological traits, such as anther position [14,15], corolla tube length [16], corolla width [17], and flower orientation [18] influence the plant's efficiency in pollen transfer or the pollinator's efficiency in obtaining nectar.

Raup [19] proposed a general framework for discovering the functional consequences of morphological variation: the theoretical morphospace paradigm. This approach explores "n-dimensional geometric hyperspaces produced by systematically varying the parameter values of a geometric form" [20]. Raup devised a simple and elegant way to describe variation in the shape of mollusk shells using a 3-parameter equation, then tested the hydrodynamic performance of artificial shells fabricated to sample a wide range of the total 3-dimensional morphospace. Because the bounds of this theoretical morphospace are not constrained by naturally existing forms, it enables unbiased study over all the theoretically possible forms, which includes those that never have occurred in nature.

Given the phenomenal diversity of flower morphologies in nature, constructing a mathematical flower model capable of quantifying and easily manipulating morphological variation along multiple orthogonal axes (morphospace) is the logical first step in our effort to distinguish between mutualistic and antagonistic plant-pollinator interactions. Following the theoretical morphospace paradigm [20], we previously defined flower morphology with a 4-parameter equation (Fig. 1A), fabricated the flower models with a 3D printer (Fig. 1B), and experimentally tested a hawkmoth pollinator's ability to exploit the flower's nectar. We showed that both flower curvature and nectary diameter influence the hawkmoth pollinator's performance [21].

In this study, we took a two-stage approach to examine the potential conflict between plants and pollinators. First, we thoroughly explored the flower morphospace along two flower shape axes (corolla curvature and nectary diameter) to search for regions which

might generate an evolutionary conflict of interest between plants and a hawkmoth pollinator. Then, we explicitly quantified the fitness of plants and hawkmoth pollinators in this critical region of morphospace by using a combination of machine vision techniques and electronic sensors to detect both the efficiency of nectar acquisition by the pollinator (a correlate of pollinator fitness) and the number of pollinator contacts with the plant's reproductive parts (a proxy for plant fitness).

Materials and Methods

(A) Animals

Individual *Manduca sexta* hawkmoths were obtained from a colony maintained by the Department of Biology at the University of Washington. Hawkmoths were flower-naïve and unfed for 1-3 days post-eclosion. The hawkmoths used in foraging experiments were obtained haphazardly with respect to sex. Each hawkmoth's sex, body weight, and proboscis length were recorded before it was used in experiments.

(B) Fabrication of artificial flowers

The artificial flowers used in this study were fabricated in polyvinyl chloride (PVC) plastic using a 3D printer by the methods described in [21]. The printed flower model was white, rigid and effectively scentless. Flower models were designed in SolidWorks (**Dassault Systèmes SolidWorks Corporation**, Waltham, Massachusetts, USA) based on an equation with four flower shape parameters: corolla curvature, nectary radius, flower length, and corolla radius. In a manner similar to that of Raup [20], we used a parametric equation for a surface generating curve [21]:

$$z(r) = L \left(\frac{r - r_0}{R}\right)^{e^c}$$

where z represents the longitudinal axis of the flower model, r represents the radial distance of the corolla from the central z-axis, c is a curvature parameter determining the lateral profile of the corolla, r_0 is the nectary radius, L is the flower length, and R is the lateral extent of the corolla from edge of the nectary to the outer lip of the flower (*i.e.*, the full radius from the central z-axis is equal to $r_0 + R$) (Fig. 1A). This curve is rotated about the z-axis and given a 1 mm thickness to create a 3D model.

(C) First stage experiment to define the critical region of flower morphospace

a. Experimental apparatus and flight arena

Artificial flowers were arranged in a 6 by 6 square array with flower centers spaced at 30.5 cm (Fig. S1). Modular T-slot extruded aluminum (80/20® Inc.) was used as the

structural support for the flower array. Each 36-flower array was populated with 6 distinct flower morphologies, present at equal frequencies. Flower positions were randomized before each foraging trial. Each artificial flower's nectar reservoir was filled with 20 μL of 20% w/v sucrose solution. The flower array was located inside a flight chamber (2.4 m width x 4.0 m length x 2.5 m height). Two dim white LED lights illuminated the arena from above, calibrated to a combined illuminance of 0.1 lux at flower level to simulate moonlight conditions. The flight chamber was also illuminated from above with a single infrared light (Magnalight LEDLB-16E-IR; 790-880 nm flat emission peak, modified by removing the light's focusing lenses to create even, diffuse lighting), invisible to *M. sexta*, to allow video recording of the hawkmoth's foraging trajectory (Fig. S1).

Each artificial flower was held in the array by a 3D-printed bracket that contained an infrared (IR) emitter-detector pair, creating an infrared beam sensor. When a hawkmoth's proboscis entered the nectar reservoir of any artificial flower, the infrared beam was broken, and this event was recorded through a data acquisition system consisting of an Arduino microcontroller (Sparkfun: DEV-11021) and a laptop computer (Fig. S1). Data collection ended when all six flowers of any single morph were exploited. An infrared-sensitive video camera was mounted above the flower array facing straight down, to capture the hawkmoth's flight trajectory as it foraged on the artificial flowers.

The air temperature of the flight arena was kept at approximately 24°C. To stimulate hawkmoth foraging, 5 μL of a 7-component synthetic scent mixture [21] was placed in the flight chamber 5 min before the experiment began. The synthetic scent mixture mimics the scents emitted by the flower of the hawkmoth-pollinated plant *Datura wrightii*.

b. Experimental treatments and sample size

A foraging trial ended when the hawkmoth left the flower array and no longer visited flowers. Foraging trials typically lasted from 4 to 12 minutes. No hawkmoth participated in more than one foraging trial. After each trial, emptied flowers were counted, empty

nectar tubes were replaced with fresh nectar tubes, and the positions of the flower morphs were re-randomized in preparation for the next foraging trial.

Hawkmoths were tested with various combinations of corolla curvature (c: $-\infty$, -4, -3, -2, -1, 0, 0.375 and 1) and nectary diameter ($2r_0$: 1, 1.75, 2.5, 3.25, 5, and 7 mm). All flowers had a length (L) of 20 mm and an overall diameter $2(R + r_0)$ of 55 mm (Fig.1B). In addition to flower exploitation data in the form of counts of emptied flower morphs, the number of visits paid to each flower morph was also recorded by analyzing the video recording of each foraging trial. Exploitation and visitation data were collected for 125 foraging trials (*i.e.*, 125 different individual hawkmoths).

c. Data analysis

Two-way analysis of variance (ANOVA) was used to test for differences in flower visitation frequency (an estimate of plant fitness, calculated as the number of times hawkmoths visit each flower morphology per trial, measured from the video captured for each foraging trial) and hawkmoth foraging success rate (an estimate of pollinator fitness, calculated as the number of emptied flowers per morphology per trial divided by the number of visits to that morphology per trial; flower morphologies which received 0 visits in a trial were excluded from foraging success rate analysis).

(D) Second stage experiments focused on the critical region of flower morphospace
a. Experimental apparatus and flight arena

In the second stage experiments, we focused on flower-hawkmoth interaction in the region of flower morphospace identified in the first stage as most sensitive to variation in corolla curvature (c) and nectary diameter ($2r_0$). In the second stage experiments, individual hawkmoths were presented with only one nectar-bearing flower in the flight arena, to examine explicitly the effectiveness of each pollinator visitation event. The experimental flower apparatus consisted of a 3D-printed flower model, an "anther/stigma" sensor assemblage to record the physical contact between the pollinator and the "reproductive parts" of the flower, and a nectary assemblage to provide nectar and detect nectar level changes (Fig. 3B).

A small (4 x 4 x 1.45 mm) 3-axis accelerometer (ADXL335, SparkFun, Niwot, Colorado, USA) was used as a proxy for the flower's reproductive organs (*i.e.,* anthers and stigma). The accelerometer was solder-connected with ultra-thin silver wire (0.14mm) and supported on a 20mm long thin stainless steel wire (0.13mm), mimicking the filament and style to support the anthers and stigma in real flowers. The other end of the steel wire was inserted into a rigid stainless steel tube to fix the free vibrating length of the wire, so that the natural frequency of the wire (about 18.4 Hz) did not change during the experiment. The accelerometer was positioned in the center of the corolla, 10 mm above the flower top plane.

A 25 mm long rigid plastic tube (inside diameter = 3.18mm) connected the printed flower and the nectary assemblage. The distance from the plane of the flower top to the bottom of nectar reservoir was 70mm, which is shorter than the average proboscis length of *M. sexta* (82.5 ± 3.25 mm, N = 58). The same infrared emitter-detector pair as in the first stage experiments was installed on the side of nectar base, allowing infrared light to pass through the bottom of the nectar reservoir to record nectar level changes. We constructed an automatic nectary refiller using a micro-injector pump, controlled by an Arduino Uno microcontroller, to push the nectar-filled Hamilton syringe with a stepper motor (adapted from [22]), to automatically replenish 20 μL of nectar during the trial. The micro-injector had enough volume capacity to refill the nectar reservoir 25 times.

The experimental flower apparatus was affixed to the floor of a flight chamber. Two distractor flowers (morphology: r_0 = 1 mm, c = -3, L = 30 mm, R = 24 mm), which had no accelerometer assemblage or nectar supply, were placed 25 cm on either side of the experimental flower. The distractor flowers were used to distract the hawkmoth from the experimental flower, so that the nectar in the experimental flower could be replenished after the hawkmoth left. A webcam (C170, Logitech, Lausanne, Switzerland) was affixed to the ceiling of the flight chamber, facing vertically down at the experimental flower. The videos were taken at a frequency of 5 frames/sec. The lighting and scent conditions in the flight chamber were identical with the first stage experiments (Fig. 3A).

b. Experimental treatments and sample size

Moths were presented with one instrumented artificial flower per trial. We tested four different corolla curvatures (c: $-\infty$, -3, -1, and 1; fixing other floral shape parameters at $2r_0 = 3$ mm; $L = 30$ mm; $R = 23.5$ mm). A 3 mm nectary diameter was used to account for the presence of the artificial anther/stigma (the diameter of the wiring is about 0.5 mm) partially occluding the corolla tube, leaving an open diameter of 2.5 mm. This diameter is consistent with measured nectary diameter values for hawkmoth-pollinated flowers such as *Petunia axillaris* and *Datura wrighttii* which have nectary diameters ranging from 1 to 2.5 mm [23]. Accelerometer and infrared nectar sensor data were collected through an Arduino Uno microcontroller at a frequency of 1 kHz. A foraging trial ended when either: 1) the nectar had been emptied 25 times (*i.e.*, reached the capacity of the micro-injector); or, 2) four minutes had passed since the last visit to the instrumented flower. For each flower morph, we collected data from 14-15 hawkmoths. The total number of hawkmoths over all trials was 58.

c. Data analysis

The videos taken by the webcam were analyzed with a customized Python program (Github repository: https://github.com/foenpeng/Controller-of-experiment-platform.git). Because the instrumented flower and webcam were both static, the hawkmoth's location in each frame can be obtained by frame subtraction. A reference frame was taken before a hawkmoth started foraging. Every new frame was subtracted from this reference frame. The centroid of the largest contour in every subtracted frame was used as an estimate of the hawkmoth's position. The coordinates of the centroid were compared with a 125 mm radius circle (about the total length of a hawkmoth's body plus a fully extended proboscis) centered on the experimental flower to determine the presence/absence of the hawkmoth pollinator. A pollinator visit was recorded whenever the hawkmoth centroid was inside the 125 mm radius.

In the second stage experiments we focused on measuring the pollinator's visit *quality*, instead of visit *quantity* as in the first stage experiments. In the second stage experiments

pollinator fitness was estimated as net rate of energy gain per visit, and plant fitness was estimated as hit counts to the artificial anther/stigma per visit. The plant's and pollinator's fitnesses (defined below) with respect to flower morphology (corolla curvature) variation were analyzed by ANOVA. The plant's and pollinator's fitnesses with respect to hawkmoth morphology (proboscis length) variation were analyzed by linear regression.

We used the amount of acquired energy (from nectar) divided by the total time spent within 125 mm of the instrumented flower during each visit to represent the pollinator's net rate of energy gain per flower visit, which is a correlate of hawkmoth fitness [24]. The total amount of time that each hawkmoth spent during each visit to the instrumented flower was calculated from the video tracking data. The amount of energy acquired is fixed for every visit: the hawkmoth always consumes all of the 20 μL of 20% sucrose nectar in the container if it reaches nectar, which provides a maximum of 64.8 J of energy assuming all energy ingested is available; if it fails to reach nectar, it obtains 0 J energy. The rate of energy expenditure is minute relative to the rate of energy gain (2-3% of acquired energy [24]), so energy expenditure is neglected.

As a proxy for the plant's fitness, the total number of "hits" on the accelerometer (representing the anthers and stigma of a real flower) during each hawkmoth visit was inferred from the accelerometer data. The analog signal readout from the accelerometer was calibrated using gravitational acceleration ($g = 9.8$ m s^{-2}) when the accelerometer was in a static state. The total acceleration was calculated as the square root of the sum of squares of acceleration in each of the three axes (x, y, z). A "hit" was identified with a peak detection algorithm (Python peaktutils package), with total acceleration greater than 3 g counted as a hit.

Results

(A) The first stage experiment identifies a critical region in flower morphospace where the interests of plants and pollinators are both sensitive to corolla curvature variation

a. Flowers with gentle curvatures are visited less frequently by hawkmoths

Flower curvature significantly influences the flower visitation frequency, the proxy for plant fitness in the first stage experiment (2-way ANOVA, p = 2.56×10^{-6}). Flowers with more extreme curvatures ($c = -\infty$ or $c = 1$) received more visits than the flowers with gentle curvatures ($c = -1$ or $c = -2$) (Fig. 2C). Nectary diameter (p = 0.31) and the interaction between nectary diameter and corolla curvature (p = 0.29) have no significant influence on flower visitation frequency.

b. Hawkmoth foraging success rate is maximized in gently-curved trumpet-shaped flowers

Foraging success rate, the proxy for pollinator fitness in the first stage experiment, is measured as the number of emptied flowers per morphology per trial divided by the total number of visits that the hawkmoth paid to that flower morphology. Two-way ANOVA shows that there is a significant effect on hawkmoth foraging success rate due to variation in nectary diameter (p = 7.18×10^{-9}), corolla curvature (p = 2×10^{-16}), and the interaction between nectary diameter and corolla curvature (p = 3.25×10^{-5}).

The easiest flower morphology for hawkmoths to exploit ($c = -3$, $2r_0 = 2.5$) yielded an average foraging success rate of 45% (± 6% SEM) while the most difficult one ($c = -\infty$, $2r_0 = 1$) was fed upon with an average success rate of 2% (± 0.7% SEM) (Fig. 2A and 2B). A peak in foraging success occurs among trumpet-shaped flowers, with the hawkmoth's performance decreasing steadily toward the extremes of corolla curvature: flat ($c = -\infty$,) and bowl-shaped ($c = 1$) flowers (Fig. 2B). The difference in foraging success rate between trumpet-shaped flowers and flowers with extreme curvatures is magnified as the nectary diameter decreases (Fig. 2B).

c. Hawkmoth foraging success rate is sensitive to curvature only when the nectary diameter is small

Individually, a large nectary diameter and a trumpet-shaped corolla curvature yield similarly high foraging success rates, at about 40% per foraging trial (Fig. 2B). Foraging performance decreases with the decrease of nectary diameter. However, poor foraging performance at a small nectary diameter (at or below 2.5 mm) can be rescued by trumpet-like curvature (c = -1 and -2) to maximal performance (Fig. 2A and 2B).

(B) The second stage experiment reveals an evolutionary conflict of interest between the plant and the hawkmoth pollinator

a. Variation in flower corolla curvature produces an evolutionary conflict

In the second stage experiment, nectary diameter was fixed at a dimension ($2r_0 = 2.5$ mm) that is relevant to naturally occurring hawkmoth-pollinated flowers [23] and also reveals the hawkmoth pollinator's sensitivity to corolla curvature (Fig. 2B). To corroborate the conflict of interest revealed by a fitness estimate related to visit *quantity* in the first stage experiments, we designed our second stage experiment to characterize visit *quality*; *i.e.* effectiveness. The plant's fitness was estimated as artificial anther/stigma hit counts per visit. The hawkmoth's fitness was estimated as the net rate of energy gain per visit. In the second stage experiment, corolla curvature significantly influences both the plant's (ANOVA, p = 1.92×10^{-10}) and the pollinator's fitness (ANOVA, p = 2×10^{-16}).

The hawkmoth's fitness is maximal for trumpet-shaped flowers (c = -1; 6.35 ± 0.22 J/s/visit SEM), and steadily decreases towards the extremes of flat ($c = -\infty$; 1.73 ± 0.19 SEM) and bowl-shaped flowers (c = 1; 2.33 ± 0.17 SEM), producing a bell-shaped fitness curve (Fig. 4A). This result is concordant with the findings from the first stage experiment when we use foraging success rate as hawkmoth's fitness measurement (Fig. 2B), and suggests that the influence of corolla curvature on hawkmoth's foraging performance is robust to the differences in experimental design and fitness measurement between first stage and second stage experiments.

The plant's fitness estimate, based on the physical contacts between the hawkmoth's body and the artificial anther/stigma (accelerometer), decreases steadily as corolla curvature increases (Fig. 4B). The bowl-shaped flower receives the fewest physical contacts ($c = 1$; 15.49 ± 0.91 hits/visit SEM), while the flat flower receives the most contacts ($c = -\infty$; 28.73 ± 3.37 SEM) (Fig. 4B).

b. Variation in hawkmoth proboscis length produces an evolutionary conflict

In addition to the engineering approach for testing for plant-pollinator conflict, we took advantage of the natural variation in hawkmoth proboscis length to evaluate its influence on plant and pollinator fitness. There is no significant difference ($p = 0.51$, two-tailed t-test) in proboscis length between male (82.19 ± 3.92 mm SD, $N = 27$) and female (82.77 ± 2.55 SD, $N = 31$) hawkmoths.

Hawkmoth proboscis length is positively correlated ($p = 0.0001$, F-test, Fig. S2A) with the hawkmoth's fitness, but negatively correlated ($p = 0.02$, F-test, Fig. S2B) with the plant's fitness.

Discussion

Although traditionally the relationship between plants and their pollinators is viewed as mutualistic, they have different requirements from their interaction: efficient pollen transfer for the plant *vs*. efficient energy acquisition for the pollinator. Using a novel combination of engineering technologies (3D printing, artificial flowers instrumented with an IR nectar sensor and an accelerometer contact sensor, automated nectar replenishment, and machine vision) to explore this interaction in flower morphospace, we have shown that these disparate requirements generate a strong conflict of evolutionary interest (Fig. 2B-C, 4A-B).

As a proof-of-concept exploration, we first examined the hawkmoth pollinator's performance in a two-dimensional flower morphospace, varying corolla curvature and nectary diameter. We showed that the influence of these two floral morphological features on pollinator performance is non-additive. Flowers with smaller nectary diameters are more difficult for the hawkmoths to exploit, but this effect could be countered by an appropriate corolla curvature (*e.g.* trumpet-shaped, $c = -1$) (Fig. 2A). The powerful morphospace paradigm [20] enabled us to study both the effects of single morphological traits and the interactions among them without bias or constraint, and we successfully demonstrated its utility by revealing a previously undiscovered interaction between corolla curvature and nectary diameter.

Corolla curvature is a key trait that significantly influences both flower visitation frequency and foraging success rates by the hawkmoth pollinator. We found that the flowers with more extreme curvatures, which are more difficult for the hawkmoths to exploit, were visited more frequently by hawkmoths (Fig. 2B-C). This result suggests that hawkmoths are unable to distinguish flower curvature differences at a distance (*e.g.*, visually), else they should preferentially visit those flower morphs that are easier to exploit, thus increasing their fitness. We suspect that when flowers are a limited resource for the pollinator, as they are in our experiments, hawkmoths make more attempts to visit the flowers whose nectar have not been emptied; *i.e.*, they may remember the location of successfully exploited flowers and avoid re-visiting them. The flowers with more extreme

curvatures are less likely to be emptied, and thus receive more visits. Since visit frequency is a component of the plant's pollination success, this result suggests an evolutionary conflict of interest between plants and their hawkmoth pollinators with respect to flower visit *quantity*: although hawkmoths obtain less energy (*i.e.,* lower pollinator fitness) from the flowers with more difficult-to-exploit curvatures, those flowers receive more visits, thus potentially increasing pollination success (*i.e.,* higher plant fitness).

To further characterize this conflict of interest between plants and pollinators, our second stage experiment used a novel approach to measure visit *quality*; *i.e.* effectiveness in the critical region of flower morphospace where hawkmoth pollinator foraging performance is exquisitely sensitive to corolla curvature. Again, we found that there is a strong conflict of fitness interest between plants and pollinators with respect to corolla curvature when using a fitness measurement based on the quality of the relevant interaction: for the plant, contact with the flower's reproductive organs (anther and stigma); and, for the pollinator, net rate of energy gain.

When corolla curvature is positive (bowl-shaped flower morphologies), the estimates of both the plant's and the pollinator's fitness are low. However, when corolla curvature is negative (trumpet to flat disc morphologies), there is a substantial conflict of interest. Although hawkmoth pollinators are less efficient at acquiring energy from the flowers with more extreme negative curvatures, the reproductive parts of those flowers receive more "hits", which is a proxy for pollen transfer (Fig. 4A-B).

This result can be understood from the mechanical basis of the two disparate activities – nectar acquisition for the pollinator *vs.* pollen transfer for the plant. On the one hand, hawkmoths rely on mechanosensory information from the proboscis to locate the nectary in low light conditions [25]. Flower corolla curvature can act as a mechanical guide to assist hawkmoth pollinators in finding the nectary [21]. The flat disc flower ($c = -\infty$) and bowl-shaped flower ($c = 1$) probably provide less passive guidance of the proboscis and more ambiguous mechanosensory information about the location of the nectary than

does the trumpet shaped corolla (c = -1). On the other hand, to deal with the more abruptly changing curvature (c = -∞ and c = -3), hawkmoths must position their heads closer to the center of flower, which leads to stronger contacts with the plant's reproductive parts (anther/stigma) (Supplementary Video S2 and S3). Gently curved flowers (c = -1) and bowl-shaped flowers (c = 1) have wider openings, with greater latitude for the position of the hawkmoth's head, so the plant's reproductive parts received fewer contacts. As a result, the intrinsic difference between the requirements of the plant and pollinator generate a strong conflict of evolutionary interest.

The conflict of evolutionary interests in corolla curvature motivated us to further explore a potential conflict by taking advantage of the natural morphological variation in the length of the hawkmoth pollinator's proboscis. Hawkmoth proboscis length has long been suspected to play a key role in flower nectar spur evolution [13], but its effects on the fitness consequences on the plants and pollinators have seldom been explicitly tested (but see [26]). When presented with flowers having an invariant corolla tube length (70 mm, from the flower top plane to the nectar reservoir) shorter than the shortest hawkmoth *M. sexta* proboscis (72 mm) in our experiment, we found that hawkmoths with longer proboscides are better at nectar feeding, but make fewer contacts with the flower's reproductive parts. The hawkmoth inserts its proboscis no further than necessary to obtain nectar [16]. A longer proboscis enables the hawkmoth to access the nectar resource with greater efficiency. However, the distance from the hawkmoth's body to the center of the flower is also greater, so the hawkmoth's body is less likely to contact the flower's reproductive parts. As a result, a longer proboscis benefits the hawkmoth while harming the plant's reproductive interests. Intuitively, a longer corolla tube or nectar spur on the flower would have the opposite effect on each party. This result corroborates previous field studies showing an evolutionary conflict between pollinator proboscis length and flower tube length [26,27]. It also lends support for the classical hypothesis that an arms race between plants and pollinators drives the evolution of long proboscides in hawkmoths and correspondingly long corolla tubes and nectar spurs in flowers [28]. Such an arms race can lead to the extreme morphologies typified by Darwin's orchid and

its hawkmoth pollinator, whose nectar spur and proboscis can be 30 cm or more in length [13].

It may be counterintuitive that the seemingly mutualistic plant-pollinator relationship could be masking underlying strong conflicts. However, there are several lines of evidence supporting the conflict hypothesis. First, conflicts of interest have been described in some obligate pollination systems, such as fig trees and fig wasps, and yucca and yucca moths [29]. Although those pollinators transfer pollen for their host plants, they also directly reproduce inside the hosts' reproductive structure, and the larvae feed on the host plant's seeds and inflorescences, which inevitably generates a fitness conflict. Second, the fossil record suggests that the earliest form of animal-vectored pollination might have evolved from pollen collecting behavior of pollen-eating insects – an antagonistic plant-herbivory interaction [1]. Nectar production by plants and nectar collection by pollinators may have evolved as a derived interaction to mitigate this strong conflict. Third, pollen deposition by pollinating animals is mostly involuntary. Cheaters exist widely in both plants and pollinators [30]. For example, 30% of orchid species have cheating strategies by either mimicking a rewarding flower (food deception) or mimicking female insects to attract naïve males (sexual deception) [31]. The legitimate pollinators of some plant species, such as hummingbirds and bumblebees, can also be nectar robbers, removing nectar through a hole pierced at the base of the flower [32] without providing pollination service to the plant.

The conflict hypothesis offers a new understanding of plant-pollinator coevolution. Notably, the rapid diversification of flowering plants – Darwin's "abominable mystery" [33] – is better understood as the result of conflict rather than mutualism, because mutualistic interactions should be maintained by stabilizing selection, reducing diversification rates. In contrast, conflict of interest could promote rapid diversification in flower morphology. The divergent selective pressure between plants and pollinators resulting from their conflict of interest will increase variation in flower morphology within a plant species. Plant populations with highly variable flower morphologies could follow different evolutionary trajectories to occupy different plant fitness peaks by

pollinator-mediated assortative mating among similar flower morphologies. Ultimately, this assortative mating could lead to plant speciation by pollinator shift – the origin of new plant species pollinated by different pollinator guilds (*e.g.*, hawkmoths, bumblebees, hummingbirds, bats) best able to exploit each alternative flower morph. The ongoing conflict between plants and their pollinators produces a coevolutionary "arms race" that never reaches equilibrium, accounting for the observed rapid plant speciation over long periods of evolutionary time.

In accordance with our finding, most cases of rapid coevolutionary diversification involve conflict of interests. For example, predator-prey [34], host-parasite [35], and even males and females involved in sexual reproduction [12] generate evolutionary arms races. Novel strategies could be favored by the antagonistic parties to counter the adaptation to each other, promoting rapid evolution on both sides of the conflict. Our results suggest that the conflict of interest between plants and pollinators might also be a prevalent and general theme in the pollination interaction. Although we recognize the cooperative aspect of pollination relationship, in terms of nectar rewards and pollen transfer service, we argue that the hidden conflict of interests between the two parties, like the evolution of corolla curvature, are more likely to promote flowering plant diversification.

The combination of 3D printing technologies, electronic sensing, and machine vision has enabled us to rationally design flower morphologies, accurately generate flower models with desired parameters, and automate high-throughput behavioral data collection during plant-pollinator interactions. Field pollination experiments could also benefit from the deployment of such engineering technologies, especially for studying night-foraging pollinators, such as hawkmoths and bats [36].

We can extend our exploration of flower morphospace to other features (*e.g.*, corolla tube length, petal number and shape, color, scent, texture), and also map the fitness landscapes of animals representing other pollinator guilds to see if the conflict found in this study is generalizable. If complemented with *in plastico* experimental evolution on artificial flower populations, we could further investigate – in real time – how the divergent

selective force exerted by different pollinator guilds drives flower pollination syndrome divergence.

Conclusion

In this study we employed a novel engineering approach to investigate a longstanding evolutionary mystery – the rapid radiation of flowering plants. Our results support the notion that a strong conflict of fitness interest exists between plant and pollinator, which could drive flower morphological diversification and contribute to plant speciation by pollinator shift.

Data Accessibility

The datasets supporting this article have been uploaded as part of the supplementary material.

Competing Interests

We have no competing interests.

Author's Contributions

F. Peng designed and carried out the second stage experiment, analyzed the data, and drafted the manuscript; E. O. Campos designed and carried out the first stage experiment, and participated in data analysis and drafting the manuscript; J.G. Sullivan participated in the second stage experiment design and execution; N. Berry and B. B. Song participated in the first stage data collection; T. Daniel and H. D. Bradshaw, Jr. conceived of the study, participated in the experimental design, and edited the draft manuscript. All authors gave final approval for publication.

References

1. Crane, P. R., Friis, E. M. & Pederson, K. R. 1995 The origin and early diversification of angiosperms. *Nature* **374**, 27–33. (doi:10.1038/374027a0)

2. Grimaldi, D. 1999 The co-radiations of pollinating insects and angiosperms in the Cretaceous. *Annals of the Missouri Botanical Garden* **86**, 373–406. (doi:10.2307/2666181)

3. van der Niet, T. & Johnson, S. D. 2012 Phylogenetic evidence for pollinator-driven diversification of angiosperms. *Trends in Ecology & Evolution* **27**, 353–361. (doi:10.1016/j.tree.2012.02.002)

4. McLaughlin, R. N. & Malik, H. S. 2017 Genetic conflicts: the usual suspects and beyond. *Journal of Experimental Biology* **220**, 6–17.

5. Hodges, S. A. 1995 The influence of nectar production on hawkmoth behavior, self-pollination, and seed production in *Mirabilis multiflora* (*Nyctaginaceae*). *American Journal of Botany* **82**, 197–204. (doi:10.1002/j.1537-2197.1995.tb11488.x)

6. Vereecken, N. J., Dorchin, A., Dafni, A., Hoetling, S., Schulz, S. & Watts, S. 2013 A pollinators eye view of a shelter mimicry system. *Ann. Bot.* **111**, 1155–1165. (doi:10.1093/aob/mct081)

7. Seymour, R. S., White, C. R. & Gibernan, M. 2003 Environmental biology: Heat reward for insect pollinators. *Nature* **426**, 243–244. (doi:10.1038/426243a)

8. Hembry, D. H., Yoder, J. B. & Goodman, K. R. 2014 Coevolution and the diversification of life. *Am Nat* **184**, 425–438. (doi:10.1086/677928)

9. Schluter, D. & McPhail, J. D. 1992 Ecological character displacement and speciation in sticklebacks. *Am Nat* **140**, 85–108. (doi:10.1086/285404)

10. Ehrlich, P. R. & Raven, P. H. 1964 Butterflies and plants: a study in coevolution. *Evolution* **18**, 586. (doi:10.2307/2406212)

11. Summers, K., McKeon, S., Sellars, J., Keusenkothen, M., Morris, J., Gloeckner, D., Pressley, C., Price, B. & Snow, H. 2003 Parasitic exploitation as an engine of diversity. *Biol Rev Camb Philos Soc* **78**, 639–675. (doi:10.1017/S146479310300616X)

12. Bonduriansky, R. 2011 Sexual selection and conflict as engines of ecological diversification. *Am Nat* **178**, 729–745. (doi:10.1086/662665)

13. Wasserthal, L. T. 1997 The pollinators of the Malagasy star orchids *Angraecum sesquipedale, A. sororium* and *A. compactum* and the evolution of extremely long spurs by pollinator shift. *Plant Biology* **110**, 343–359. (doi:10.1111/j.1438-8677.1997.tb00650.x)

14. Conner, J. K., Sahli, H. F. & Karoly, K. 2009 Tests of adaptation: functional studies of pollen removal and estimates of natural selection on anther position in wild radish. *Ann. Bot.* **103**, 1547–1556. (doi:10.1093/aob/mcp071)

15. Harder, L. D. & Barrett, S. C. H. 1993 Pollen removal from tristylous *Pontederia cordata*: effects of anther position and pollinator specialization. *Ecology* **74**, 1059–1072. (doi:10.2307/1940476)

16. Nilsson, L. A. 1988 The evolution of flowers with deep corolla tubes. *Nature* **334**, 147–149. (doi:10.1038/334147a0)

17. Muchhala, N. 2015 Adaptive trade-off in floral morphology mediates specialization for flowers pollinated by bats and hummingbirds. *Am Nat* **169**, 494–504. (doi:10.1086/512047)

18. Ushimaru, A., Dohzono, I., Takami, Y. & Hyodo, F. 2009 Flower orientation enhances pollen transfer in bilaterally symmetrical flowers. *Oecologia* **160**, 667–674. (doi:10.1007/s00442-009-1334-9)

19. Raup, D. M. 1966 Geometric analysis of shell coiling: general problems. *Journal of Paleontology* **40**, 1178–1190. (doi:10.2307/1301992)

20. McGhee, G. R. 2006 *The geometry of evolution*. Cambridge: Cambridge University Press. (doi:10.1017/CBO9780511618369)

21. Campos, E. O., Bradshaw, H. D. & Daniel, T. L. 2015 Shape matters: corolla curvature improves nectar discovery in the hawkmoth *Manduca sexta*. *Funct Ecol* **29**, 462–468. (doi:10.1111/1365-2435.12378)

22. Wijnen, B., Hunt, E. J., Anzalone, G. C. & Pearce, J. M. 2014 Open-source syringe pump library. *PLoS ONE* **9**, e107216. (doi:10.1371/journal.pone.0107216)

23. Campos, E. O. 2017. *Plant-pollinator interactions in an ecological and evolutionary context: the promising role of 3D-printing technology and mathematical modeling* (Doctoral dissertation). Retrieved from WorldCat database. (OCLC No.: 1014344606)

24. Sprayberry, J. D. H. & Daniel, T. L. 2007 Flower tracking in hawkmoths: behavior and energetics. *Journal of Experimental Biology* **210**, 37–45. (doi:10.1242/jeb.02616)

25. Goyret, J. & Raguso, R. A. 2006 The role of mechanosensory input in flower handling efficiency and learning by *Manduca sexta*. *Journal of Experimental Biology* **209**, 1585–1593. (doi:10.1242/jeb.02169)

26. Pauw, A., Stofberg, J. & Waterman, R. J. 2009 Flies and flowers in Darwin's race. *Evolution* **63**, 268–279. (doi:10.1111/j.1558-5646.2008.00547.x)

27. Anderson, B. & Johnson, S. D. 2008 The geographical mosaic of coevolution in a plant-pollinator mutualism. *Evolution* **62**, 220–225. (doi:10.1111/j.1558-5646.2007.00275.x)

28. Micheneau, C., Johnson, S. D. & Fay, M. F. 2009 Orchid pollination: from Darwin to the present day. *Botanical Journal of the Linnean Society* **161**, 1–19. (doi:10.1111/j.1095-8339.2009.00995.x)

29. Dufay, M. & Anstett, M.C. 2003 Conflicts between plants and pollinators that reproduce within inflorescences: evolutionary variations on a theme. *Oikos* **100**, 3–14. (doi:10.1034/j.1600-0706.2003.12053.x)

30. Ghoul, M., Griffin, A. S. & West, S. A. 2014 Toward an evolutionary definition of cheating. *Evolution* **68**, 318–331. (doi:10.1111/evo.12266)

31. Selosse, M.A. 2014 The latest news from biological interactions in orchids: in love, head to toe. *New Phytologist* **202**, 337–340. (doi:10.1111/nph.12769)

32. Irwin, R. E., Bronstein, J. L., Manson, J. S. & Richardson, L. 2010 Nectar robbing: ecological and evolutionary perspectives. *Annu. Rev. Ecol. Evol. Syst.* **41**, 271–292. (doi:10.1146/annurev.ecolsys.110308.120330)

33. Friedman, W. E. 2009 The meaning of Darwin's 'abominable mystery'. *American Journal of Botany* **96**, 5–21. (doi:10.3732/ajb.0800150)

34. Geffeney, S., Ruben, P. C. & Brodie, E. D. 2002 Mechanisms of adaptation in a predator-prey arms race: TTX-resistant sodium channels. *Science* **297**, 1336–1339. (doi:10.1126/science.1074310)

35. Spottiswoode, C. N. & Stevens, M. 2012 Host-parasite arms races and rapid changes in bird egg appearance. *Am Nat* **179**, 633–648. (doi:10.1086/665031)

36. Nachev, V., Stich, K. P., Winter, C., Bond, A., Kamil, A. & Winter, Y. 2017 Cognition-mediated evolution of low-quality floral nectars. *Science* **355**, 75–78. (doi:10.1126/science.aah4219)
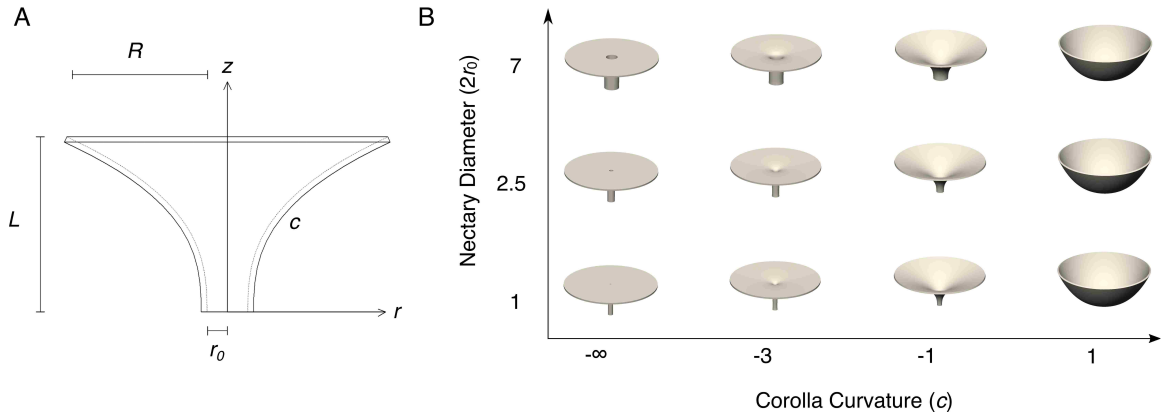
Figure 1. Design of artificial flowers. (A). Side view of a flower, showing the four parameters in the equation. (B). 3D rendering of some representative flowers with variation in nectary diameter and corolla curvature. The corolla tube length L is fixed at 20 mm and the overall diameter $2(R + r_0)$ is fixed at 55 mm.
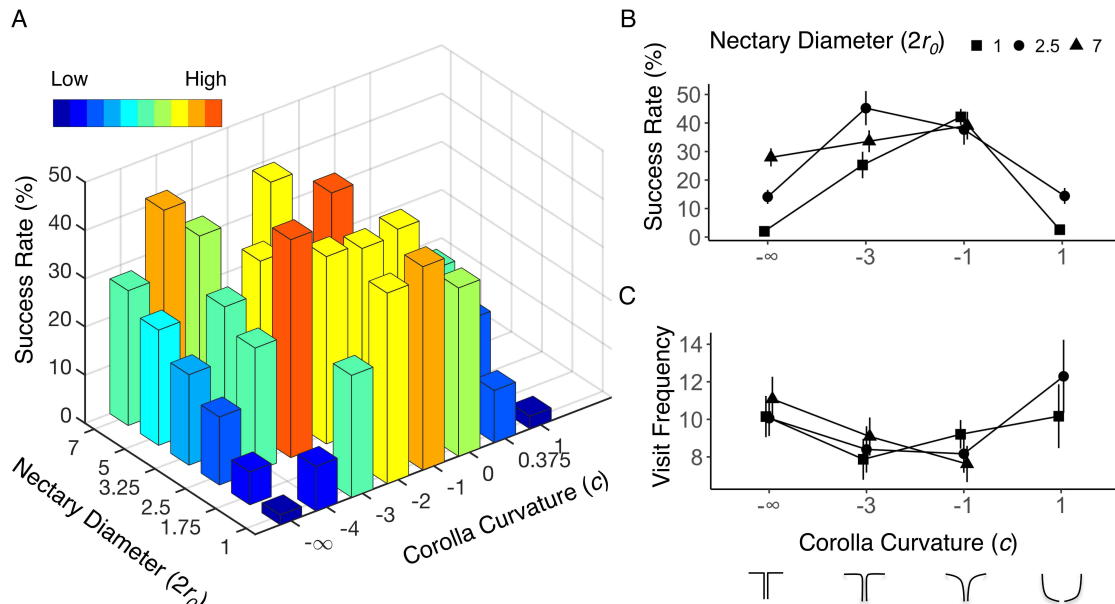
Figure 2. Hawkmoth foraging success rate and flower visitation frequency in the first stage experiment. (A). Hawkmoth foraging success rate (number of emptied flower/number of visits per trial, a correlate of pollinator fitness) across two dimensions of flower morphospace. Graphs B and C show some flowers that capture the range of variation along the two morphological axes from the full data set (Supplementary Table 1). (B). Hawkmoth foraging success rate. (C) Flower visitation frequency. Error bars represent ± 1 standard error of the mean (SEM).
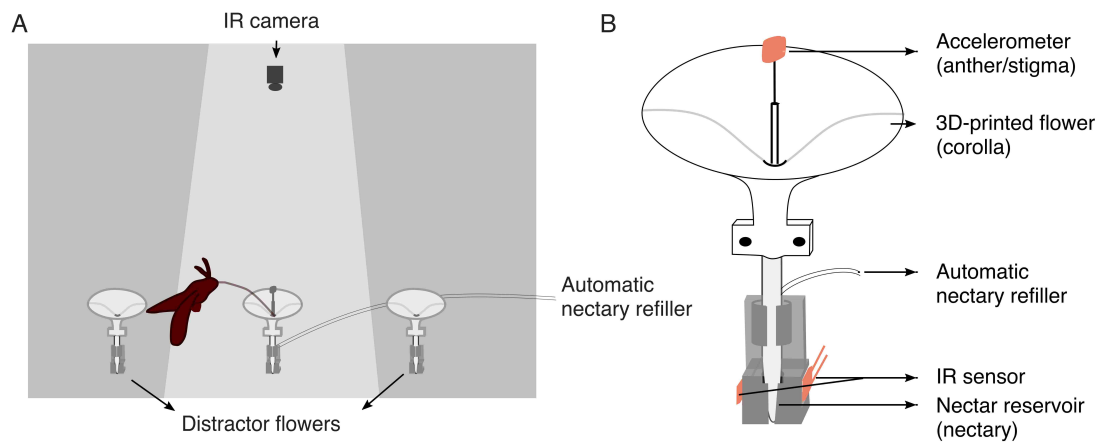
Figure 3. Second stage experimental setup. (A). Hawkmoth flight chamber. Only the center flower is instrumented and supplied with nectar. The flowers on the two sides are distractors. (B). Instrumented flower model, which is an enlarged view of the center flower in (A).
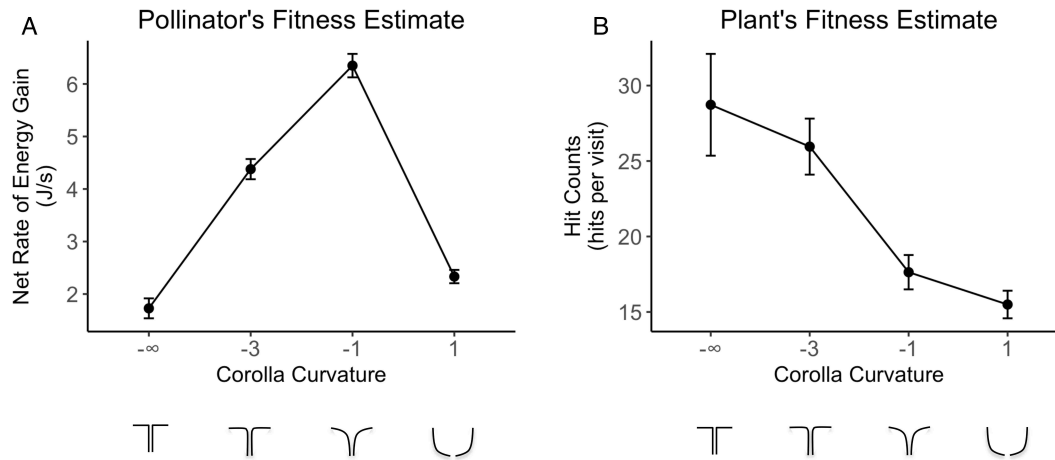
Figure 4. The fitness of pollinator and plant in the critical region of flower morphospace. (A). Hawkmoth pollinator's fitness measured as net rate of energy gain; (B). Plant's fitness measured as hit counts to the artificial anther/stigma. Error bars are ±1 SEM. Sample size (number of visits) of each flower morph is: $c = -\infty$, N = 198; $c = -3$, N = 428; $c = -1$, N = 384; $c = 1$, N = 806.

Chapter 3

Comparing pollination performance between hawkmoths and hummingbirds with 3D printing, automated sensing, and machine vision

Foen Peng, Joseph Garret Sullivan, Thomas L. Daniel, and H. D. Bradshaw, Jr.*

Department of Biology, University of Washington, Seattle, Washington 98195, USA

* Correspondence: toby@uw.edu

Abstract

Pollinator-mediated selection is an important factor that drives plant speciation. Although it is suggested that the phenotypic differences among different pollinator groups, such as insects and birds, can affect their interactions with flowers, few studies have rigorously examined the impact on both the plant's and pollinator's fitness. In this experiment, I presented 3D-printed flowers with variation in corolloa curvature and petal reflexing to two pollinators, hawkmoths and hummingbirds. I used electronic sensors to measure the proxies of the plant's and pollinator's fitness: frequency of physical contacts with the plant's reproductive parts and the pollinator's rate of energy gain *via* nectar consumption. Corolla curvature generates a strong conflict between the fitness interests of the hummingbird and the plant. But, in contradiction to a previous study, it does not do so for the hawkmoth, probably because a large nectary diameter reduces the difficulty for the hawkmoth to handle flowers with challenging curvature. Petal reflexing does not have a strong impact on fitness of either partner, but it greatly reduces the occurrence of hummingbird perching while feeding, so petal reflexing could be a deterrent mechanism to avoid pollinators which require a landing platform, such as bees. I demonstrated that 3D printing and engineering technologies can offer new insights in the centuries-old field of pollination biology.

Introduction

Animal pollinators encompass diverse animal lineages, such as insects (*e.g.,* bees, moths, and butterflies), birds (*e.g.,* hummingbirds, sunbirds), and mammals (*e.g.,* bats). Although different groups of animal pollinators vary in morphology, behavior, and physiology, they are all involved in two essential processes of pollination: resource exploitation and pollen transfer. The phenotypic differences among different pollinator guilds are likely to have profound impacts on the efficiency of resource exploitation and pollen transfer.

It has been hypothesized that a plant species adapts to its most efficient pollinator guild, and pollinator shift to a different guild can lead to divergence in floral traits and subsequence speciation as a result of pollinator-mediated assortative mating (Fenster et al. 2004). Although the differences in pollinator preference and performance were appreciated intuitively, few experiments have rigorously quantified and compared their effects on both the plant's and the pollinator's fitness. A major difficulty is to have different pollinators visit a common set of flowers with morphological variation of interest. Thus there is a gap in our conceptual understanding of pollinator-mediated ecological speciation in flowering plants.

Using 3D-printed artificial flowers as experimental subjects has a unique advantage in testing the fitness differences among different pollinator groups. Natural flowers, even when from closely related taxa, usually differ in multiple traits that have evolved as adaptations to different pollinators. Genetic crossing or genetic engineering can generate combinations of different floral traits, but even these approaches can be confounded because of genetic linkage or pleiotropic effects of the transgene. Additionally, it is difficult to tease apart the effects of different floral traits on pollination performance. In contrast, 3D-printing allows us to generate combinatorial floral traits without constraints or bias, and the effects of different floral traits can be examined independently or in combination.

I used a similar approach to that described in Chapter 2 to compare the performance of two pollinators, hawkmoths and hummingbirds, which are very different in terms of

phylogenetic distance, morphology, and behavior. Also, adaptive divergence or speciation events driven by selection by these two pollinators are inferred in many closely related species of flowering plants (Streisfeld and Kohn 2007; Whittall and Hodges 2007). Some floral traits serving to attract (*e.g.,* color and scent) or reward (*e.g.,* nectar quantity) pollinators were shown to be important in discriminating between the two pollinator guilds. For example, hawkmoth-pollinated flowers are usually white and scented, but hummingbird-pollinated flowers are usually red and scentless (Fenster et al. 2004). However, the effects of floral traits important in pollination performance, such as flower corolla shape, have rarely been studied.

In this experiment, I examined the effects of corolla shape variation along two axes: corolla curvature and petal reflexing. Corolla curvature was shown in Chapter 2 as a key trait that influences both the plant's and the hawkmoth pollinator's fitness, but its impact in the fitness of hummingbird pollination is unknown. Petal reflexing is a trait that is usually observed in hummingbird-pollinated flowers (Cronk and Ojeda 2008). It is hypothesized as a pollinator avoidance mechanism to deter unwanted pollinators which require a landing platform, such as bees, and to avoid pollen loss. This hypothesis has not been tested empirically and it is unknown whether this trait also positively improves hummingbird's efficiency in pollen transfer or nectar exploitation.

The goals of this study are: *a.* to examine whether the conflict of interest identified in Chpater 2 is a general phenomenon that also exists in other pollination systems; *b.* to explore how the conflict of interest in one trait is affected by the combinatorial effects of other traits; *c.* to identify regions of flower morphospace that could discriminate the two pollinators and potentially drive pollinator-mediated divergence.

Materials and methods
(A). Mathematically defined flower morphology
I used an extended version of the equation in (Campos et al. 2015) to define flower morphology. Besides the 4 parameters (L, r_0, R, and c) in the original equation, I also defined p as the degree of petal reflexing. The extended equation is:

$$z(r) = L \left(\frac{r - r_0}{R}\right)^{e^c} - \left(\frac{2(r - r_0)}{R}\right)^{p}$$

where z represents the longitudinal axis of the flower model, r represents the radial distance of the corolla from the central z-axis, c is a curvature parameter determining the lateral profile of the corolla, r_0 is the nectary radius, L is the flower length, R is the lateral extent of the corolla from edge of the nectary to the outer lip of the flower (*i.e.*, the full radius from the central z-axis is equal to $r_0 + R$), and p is the degree that the outer half of the corolla curve reflexing down (Fig. 1A). This curve was rotated about the z-axis and given a 2 mm thickness to create a 3D model. The method of 3D-printing artificial flowers was identical to (Campos et al. 2015).

Petal reflexing had a relatively large impact on the outside half of the corolla curve (*i.e.* where $r > R/2 + r_0$), but its impact on the curvature of inside half is minimal (*i.e.* where $r < R/2 + r_0$) (Fig. 1A). Nine flowers with various combinations of corolla curvature (c: -1, -2, -3) and petal reflexing (p: 0, 3, 4) were tested in this experiment (Fig. 1B). Other parameters were fixed ($L = 20$cm, $r_0 = 2.5$ cm, and $R = 22.5$ cm). The flower morphologies used for hawkmoth and hummingbird pollination experiments were the same.

(B) Pollination experiment with the hawkmoth pollinator

1. Experimental apparatus and flight arena

The experimental apparatus was identical to the previous experiment (Chapter 2). Briefly, the experimental apparatus consisted of a 3D-printed flower model, an "anther/stigma" sensor (using a small accelerometer) assemblage to record the physical contact between the pollinator and the reproductive parts of the flower, and a nectary assemblage to provide a fixed amount of nectar (20 μl 20% weight/volume sucrose solution) for each visit and to detect nectar level changes (using an infrared light sensor).

The artificial flower was put in an orientation such that the central axis (z-axis) of flower formed a 30° angle with the ground surface. All other flight arena settings were the same

with the previous hawkmoth experiment (Chapter 2). Briefly, hawkmoths were put in an enclosed dark flight chamber to simulate the night environment. Artificial flower scent mixture (5 μl) was added to the bottom of the chamber to initiate hawkmoth's feeding behavior. A small LED was placed on the ceiling of the flight chamber to provide about 5 lux luminance for moth foraging. An infrared light, which moths cannot see, was placed on the ceiling to provide illumination for video recording. A webcam (C170, Logitech, Lausanne, Switzerland) with the infrared light filter removed was used to record the moth's activity. A custom-fabricated micro-injector was used to replenish the sucrose nectar solution (20 μl) in the flower's nectar reservoir after each visit.

2. Experimental treatment and sample size

I used lab-reared night-foraging hawkmoths (*Manduca sexta*) for the pollination experiments. The hawkmoths were 1-3 days after eclosion, unfed, and naïve to flowers. A new hawkmoth was used in each experiment trial. I tested each flower morphology with 6-11 experimental trials (*i.e.,* 6-11 hawkmoths). The total number of hawkmoths used in the experiment was 62.

3. Data analysis

Analysis of hawkmoth pollination data was described in Chapter 2. Briefly, I used a background subtraction Python program to analyze the video and quantify the duration of each visit. I defined the hawkmoth's fitness as the rate of energy gain, which was the total amount of energy acquired by the moth (64.8 J if the moth emptied the nectar, or 0 J if the moth failed to reach the nectar; the moth always drank all of the nectar if it successfully reached the nectar reservoir) divided by the amount of time the moth spent during each visit. I defined the plant's fitness as the total number of hits on accelerometer during each visit. The fitness data along the corolla curvature and petal reflexing axes were analyzed with two-way ANOVA.

(C) Pollination experiment with the hummingbird pollinator
1. Experimental apparatus and flight arena

In the hummingbird experiment, the 3D-printed flower model and "anther/stigma" (accelerometer) sensor assemblage were identical to the one used for the hawkmoth experiment. I used a commercially available hummingbird feeder (Perky-Pet 203CPBN) to provide nectar, rather than using the custom-fabricated nectar assemblage. The 4 flowers originally installed in the commercial feeder were removed. I sealed 3 feeding tubes of the feeders with hot melt glue and left only 1 feeding tube open. Then I attached the base of my experimental apparatus directly to the open tube. The infrared light sensor, which was fixed to the side of flower base, detected the events when the hummingbird's tongue blocked the light beam during its visit to the apparatus.

I built a $1m^3$ cube with modular T-slot extruded aluminum (80/20® Inc.) to provide structural support for the apparatus, which was set on the roof (*ca*. 25m above ground level) of Kincaid Hall on the University of Washington campus. The feeder was presented in the center of the cube. A webcam (C170, Logitech, Lausanne, Switzerland) was fixed on one face of the cube (0.5 m away from the feeder) to record the hummingbirds' visits. A white foam board was put on the opposite face of the cube to provide a high-contrast background. A customized motion detection Python program based on frame subtraction (Github repo: https://github.com/foenpeng/Hummingbird-experiment) was used to detect the presence or absence of hummingbirds. Data from the webcam, the accelerometer, and the infrared light sensor were written to disk only when a hummingbird was present.

2. Experimental treatment and sample size

The hummingbirds used in the experiment were free-living Anna's hummingbirds (*Calytpe anna*) on the University of Washington Seattle campus. Sucrose solution (20% weight/volume) was used as nectar. In each day, experiments started at sunrise and ended at sunset. I ran the experiment for 121 days from the late May to mid-October 2017. For each flower morphology, I collected data for 8-28 days.

3. Data analysis

I used a machine vision program (Github repo: https://github.com/foenpeng/Bird-data-

analysis) to retrieve the contour of hummingbird for each video frame. I defined each visit as the time during which the bird's contour was inside the flower's top plane. In order to distinguish authentic visits from occasional flybys, only visit durations equal to or greater than 0.3 seconds (*i.e.,* at least 3 consecutive frames satisfying conditions) were considered a visit. Occasionally, hummingbirds fed on the apparatus by standing on the corolla. The ABS plastic printing material provided stable support for hummingbirds to perch on flower corolla, which rarely happens in natural flowers. So, I used a support vector machine (SVM) classifier (Github repo: https://github.com/foenpeng/Bird-data-analysis) to distinguish the hummingbird's perching *vs.* hovering behavior in each frame based on the bird's contour, which gave an F1 score (the harmonic average of the precision and recall) of 0.98. Only hovering visits without perching frames were analyzed. The relationship between floral features (corolla curvature and petal reflexing) and the occurrence of the hummingbird's perching visit was analyzed by Chi-squared test.

I applied a peak detection algorithm on the infrared light sensor data to measure the number of hummingbird tongue licks per visit. In order to estimate the volume of nectar that the hummingbird acquired per lick, I did a pilot experiment by feeding hummingbirds with 100 µl of nectar in a PCR tube and counting how many licks it took to empty all the nectar. In my pilot experiment, hummingbirds obtained about 1.89 µl of 20% sucrose per lick, which provided 6.12 J of energy.

The rate of energy gain was used as a proxy for hummingbird's fitness, which was calculated as the amount of energy gain per visit divided by the visit duration.

Plant fitness was estimated as accelerometer hit counts per visit, as in the hawkmoth experiment. Data were analyzed by two-way ANOVA.

Results
(A) Corolla reflexing affects hummingbird perching on artificial flowers
I recorded 6514 hummingbird visits, of which 950 contained at least one video frame with perching behavior based on the SVM classifier. These visits were excluded in the

subsequent fitness analysis. Both corolla curvature (p < 2e-16, Chi-squared test) and petal reflexing (p < 2e-16, Chi-squared test) influence whether hummingbirds perch or hover when visiting artificial flowers. Flowers without petal reflexing ($p = 0$) have a large proportion of perching visits (39.7%), while flowers with petal reflexing greatly reduce the occurrence of perching ($p = 3$: 4.2% and $p = 4$: 2.6%). Flowers with gentle curvature ($c = -1$) also receive more perching visits (23.67%) than flowers with more abrupt curvature ($c = -2$: 11.3% and $c = -3$: 11.8%) (Fig. 2).

(B) Hummingbirds and plants have a strong conflict of interest over corolla curvature evolution, but not petal reflexing evolution

Corolla curvature strongly influences the hummingbirds' fitness (p = 2e-16, two-way ANOVA). When corolla curvature changes from gently-curved ($c = -1$) to abruptly-curved ($c = -3$), the hummingbird's fitness decreases. Petal reflexing also significantly influences the hummingbird's fitness (p = 2e-8, two-way ANOVA), with higher fitness when feeding from flowers with petal reflexing ($p = 3$: 20.2 J/s, and $p = 4$: 20.0 J/s) than flowers with no reflexing ($p = 0$: 15.5 J/s). Also, petal reflexing can alleviate the difficulty for hummingbirds to feed on abruptly curved flowers (p = 1e-7, interaction term in the two-way ANOVA). Overall, the highest hummingbird fitness in my experiment is 31.1 ± 0.9 J/s SEM ($c = -1$ and $p = 3$), while the lowest fitness is 10.3 ± 0.4 J/s ($c = -3$ and $p = 3$) (Fig. 3A).

Corolla curvature also affects the plant's fitness (p = 2e-16, two-way ANOVA). When corolla curvature changes from gently curved ($c = -1$) to more curved ($c = -2$), the plant's fitness increases, but further increase in curvature (-2 to -3) does not increase the plant's fitness. Petal reflexing does not have a significant impact on plant's fitness (p = 0.084, two-way ANOVA). Overall, the highest plant fitness is 2.2 ± 0.2 hits per visit ($c = -2$ and $p = 3$), while the lowest plant fitness is 0.03 ± 0.01 ($c = -1$ and $p = 0$) (Fig. 3B).

(C) Hawkmoths and plants do not have a strong conflict of interest over either corolla curvature or petal reflexing evolution

We recorded 1299 hawkmoth visits in total, of which 1128 visits resulted in the hawkmoth successfully reaching the nectar.

Corolla curvature has a weak but significant influence on the hawkmoth's fitness ($p = 0.03$, two-way ANOVA). Petal reflexing alone does not significantly impact the hawkmoth's fitness ($p = 0.43$, two-way ANOVA), but increased petal reflexing can reverse the effects of corolla curvature ($p = 1e-7$, interaction term in the two-way ANOVA). The highest hawkmoth fitness is 7.3 ± 0.4 J/s SEM ($c = -1$ and $p = 4$), while the lowest is 5.4 ± 0.3 J/s ($c = -3$ and $p = 0$) (Fig. 3C)

Corolla curvature has a significant influence on plant's fitness, as well ($p = 3e-11$, two-way ANOVA). Flowers with abruptly curved corollas ($c = -3$) have higher fitness than flowers with gently curved corollas ($c = -1$). Petal reflexing does not significantly influence the plant's fitness ($p = 0.14$, two-way ANOVA). The interaction between corolla curvature and petal reflexing is significant ($p = 0.01$, two-way ANOVA). Overall, the highest plant fitness is 30.7 ± 3.4 hits per visit, while the lowest plant fitness is 10.0 ± 1.4 hits per visit (Fig. 3C).

Discussion

Motivated by the strong evolutionary conflict between plants and their hawkmoth pollinators discovered in the previous study (Chapter 2), I applied similar approaches in this experiment on two different pollinators – hummingbirds and hawkmoths. Interestingly, hummingbirds also showed a strong conflict of interest with plants over corolla curvature evolution: gently curved ($c = -1$) flowers favor the hummingbird's fitness but moderate ($c = -2$) or abruptly ($c = -3$) curved flowers favor the plant fitness. Flowers with abrupt or moderate curvature also have narrow openings at the throat of corolla (Fig. 1), so the hummingbird's head is forced to contact plant's anthers and stigma, which increases the possibility of pollen transfer, thus increasing plant fitness.

Interestingly, the plant's fitness plateaus or decreases when curvature changes from moderate to abrupt, which suggests that the plant's fitness is only sensitive to curvature

when change is in the gentle range. Why the gently curved flower is easier for hummingbirds to feed on is less clear. Unlike night-foraging hawkmoths, hummingbirds have a sophisticated visual system, so the mechanosensory information that corolla curvature provides to hawkmoths should play a minimal role in hummingbird pollination. Maybe the narrow opening in abruptly curved flowers keeps the hummingbird's body further away from the nectar reservoir, so the hummingbird has to extend its tongue further to get enough nectar, which could reduce the frequency of licks, thus reducing the rate of energy gain.

Petal reflexing is a floral feature that is usually observed in hummingbird-pollinated flowers (Bradshaw and Schemske 2003; Cronk and Ojeda 2008). In my experiment, this feature does not significantly improve the plant's fitness. Petal reflexing can moderately improve the hummingbird's feeding efficiency, but the effect is not as strong as corolla curvature (Fig. 3A). The evolution of petal reflexing in hummingbird pollinated plants could also be explained by avoidance of pollen waste resulted from visits of other unwanted pollinators which require a landing platform, such as bees (Gegear et al. 2017). And although hummingbirds hover when pollinating natural flowers (Cronk and Ojeda 2008), they are able to perch on the solid artificial flowers in my experiment when there is no petal reflexing. Flowers with petal reflexing force the pollinator to hover when visiting. So petal reflexing could be an effective strategy to deter unwanted pollinators which require a landing platform (Fig. 2).

In the hawkmoth experiment, corolla curvature no longer poses a strong conflict between plant and pollinator, in contrast to the results from Chapter 2. The change of corolla curvature from gently-curved to abruptly-curved increases plant fitness, which is consistent with previous experiments (Chapter 2). However, although previous experiments (Chapter 2) showed that increasing corolla curvature decreases the hawkmoth's fitness, I did not find a similar trend in this experiment. Although there are differences in the hawkmoth's fitness among the different flower morphologies, in general the hawkmoth's fitness stays at a high plateau. This inconsistency can be explained by the difference in flower nectary diameter. I showed in previous experiments

that large nectary diameter could rescue the hawkmoth's poor performance when visiting flowers with abrupt corolla curvatures (Chapter 2). In this experiment, I used a large nectary diameter ($2r_0$ = 5mm, instead of $2r_0$ = 3mm) for both hawkmoth (proboscis diameter: ~ 1mm) and hummingbird (beak diameter: ~ 3mm) experiment, to make sure that the nectar was accessible to both pollinators, thus lowering the difficulty for hawkmoths to find nectar. Consequently, the hawkmoth's fitness is relatively high among all the flower morphologies tested in this study. Interestingly, this result suggests that strong evolutionary conflict in one trait (corolla curvature) can be mitigated by the compounding effects of another trait (nectary diameter). This finding stresses the importance of studying the combinatorial effects of multiple traits.

Overall, neither corolla curvature nor petal reflexing discriminate between hummingbird and hawkmoth pollinators in these experiments. The two pollinator guilds differ in an array of traits, such as morphology (*e.g.,* relatively short beak *vs.* long proboscis) and behavior (*e.g.,* diurnal foraging *vs.* nocturnal foraging). Future experiments with additional combinations of floral traits, such as nectary diameter and corolla tube length, can enrich our understanding of how floral traits might lead to speciation by pollinator shift.

The combination of 3D printing to generate floral traits, electronic sensing to estimate fitness, and machine vision to analyze animal behavior provides a powerful, unbiased, unconstrained methodological platform for future pollination biology research. In this experiment, I demonstrated its versatility by exploring the pollination fitness landscapes of different pollinator guilds through functional tests on a common region of floral morphospace.

References

Bradshaw, H. D., and D. W. Schemske. 2003. Allele substitution at a flower colour locus produces a pollinator shift in monkeyflowers. Nature 426:176–178.

Campos, E. O., H. D. Bradshaw, and T. L. Daniel. 2015. Shape matters: corolla curvature improves nectar discovery in the hawkmoth Manduca sexta. Funct. Ecol. 29:462–468.

Cronk, Q., and I. Ojeda. 2008. Bird-pollinated flowers in an evolutionary and molecular context. J. Exp. Bot. 59:715–727.

Fenster, C. B., W. S. Armbruster, and P. Wilson. 2004. Pollination syndromes and floral specialization. Annu. Rev. Ldots.

Gegear Robert J., Burns Rebecca, and Swoboda-Bhattarai Katharine A. 2017. "Hummingbird" floral traits interact synergistically to discourage visitation by bumble bee foragers. Ecology 98:489–499.

Streisfeld, M., and J. Kohn. 2007. Environment and pollinator-mediated selection on parapatric floral races of Mimulus aurantiacus. J. Evol. Biol. 20:122–132.

Whittall, J. B., and S. A. Hodges. 2007. Pollinator shifts drive increasingly long nectar spurs in columbine flowers. Nature 447:706–709.
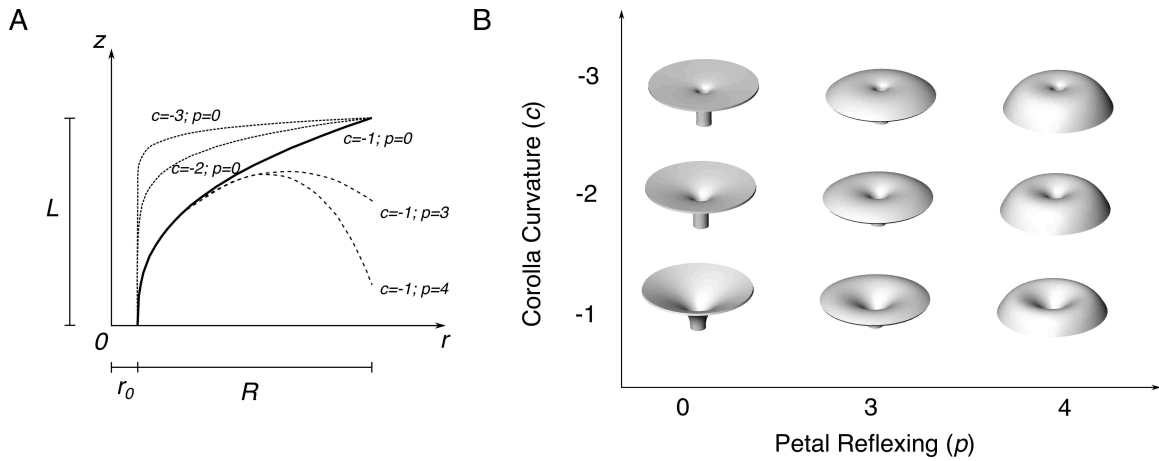
Figure 1. Design of artificial flowers.

A. The parameters used to define the flower-generating curve. B. 3D-rendering of flowers with variation along corolla curvature and petal reflexing axes. The solid line in the center of A shows the curve of the flower on the lower left of B ($c = -1$; $p = 0$). The densely dotted lines in A (above solid line) show variation along the corolla curvature axis in B. The sparsely dotted lines in A (below the solid line) show variation along the petal reflexing axis in B.
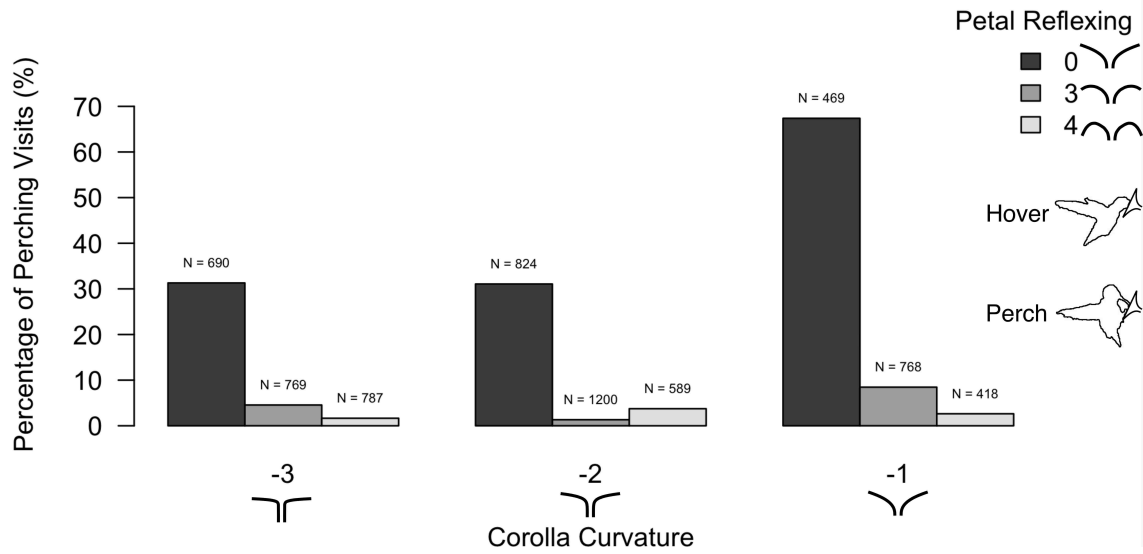
Figure 2. Percentage of hummingbirds' perching visits

The hummingbird silhouettes in the legend show two different behavioral types of visit: hovering and perching. The percentage of perching visits for each morphology is calculated by comparing the number of perching visits with the number of total visits to particular flower morphology (indicated as the numbers on the top of each bar).
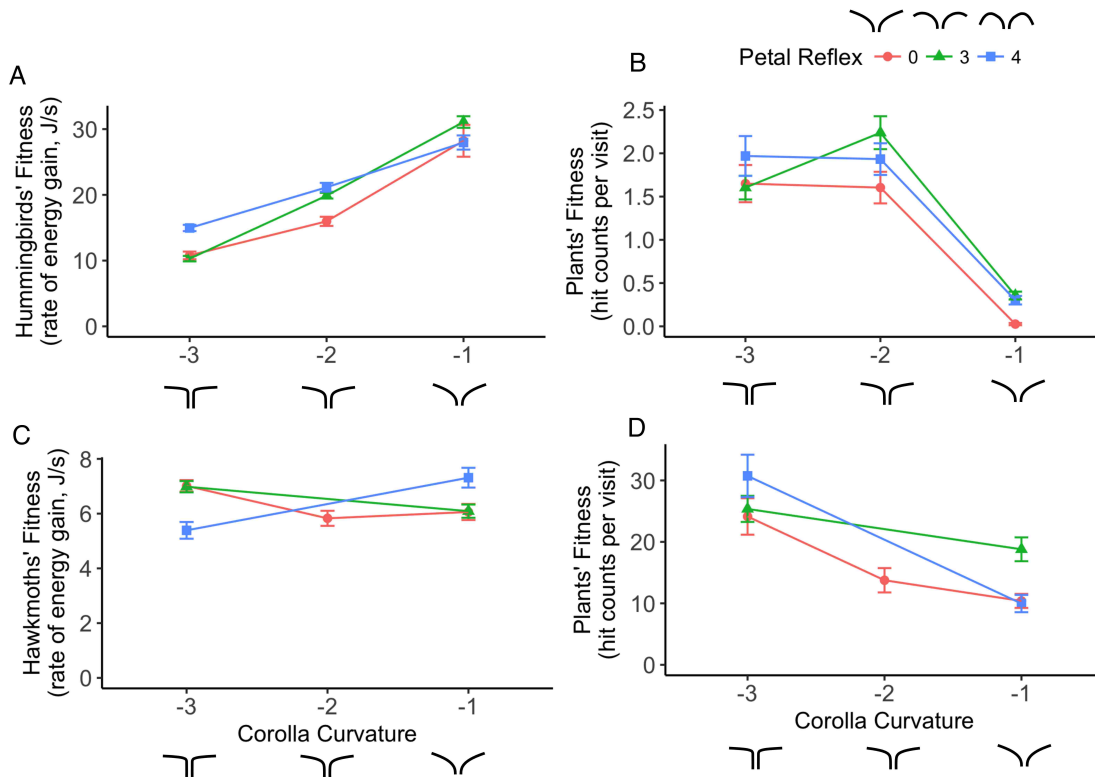
Figure 3. Animal and plant fitness estimate

A and B show the hummingbird's and plant's fitness in the hummingbird pollination experiments, respectively. C and D show the hawkmoth's and plant's fitness in the hawkmoth pollination experiment,s respectively. Variation in corolla curvature is indicated on the horizontal axes. Variation in petal reflexing is indicated with the different colors and symbols. Error bars are SEM.

Chapter 4

Hidden conflicts in cooperation – a driver of diversification

Foen Peng*

Department of Biology, University of Washington, Seattle, Washington 98195, USA

* Correspondence: peng.foen@gmail.com

Abstract

Cooperative biological interactions, such as sexual reproduction and animal pollination, are fundamental constructive forces that shape the planet's biodiversity. However, the mechanism by which cooperative interactions influence the diversification process is still enigmatic. Theoretically, cooperative interactions should hinder diversification through stabilizing selection on the phenotypes of mutual benefit. However, rapid diversifications are often observed in cooperatively interacting groups in nature. In this paper, I highlight the ubiquitous existence of conflicts of interest within cooperative interactions, and suggest that the conflicts of interest in cooperative interactions can promote diversification. I also identify future directions that could strengthen our understanding of the diversification of cooperatively interacting groups.

Diversification with cooperative interactions: a paradox

Darwin considered the sudden origination and explosive diversification of flowering plants (angiosperms) an "abominable mystery" in earth's evolutionary history [1]. The *ca*. 400,000 extant species of flowering plants represent one-quarter of multicellular species described by science. The ubiquitous biological interactions between plants and animals, including both antagonistic interactions such as parasitism and herbivory, and cooperative interactions such as seed dispersal and pollination, are frequently invoked as an explanation for the mystery of flowering plant diversification [2,3].

Ehrlich and Raven [2] showed that the antagonistic plant-herbivore interaction can drive evolutionary diversification of both sides of the interaction. Animal herbivory is a threat to the host plant's survival, and the defensive toxic secondary metabolites produced by the host plant harm the herbivores. This inherent conflict of interest can drive evolutionary "arms races" – recurring adaptation by one party and counteradaptation by the other. A new adaptation of the host plant's defense mechanism can create an enemy-free space, allowing the host plant to diversify and explore new ecological opportunities. Follow-on counterdefense adaptation enables the herbivore to radiate and exploit new plant resources. Therefore, this "arms race" generated by conflicts of interest can drive the rapid diversification of both plant and herbivore. Similarly, many rapid diversifications driven by conflicts of interest have also been observed in other antagonistic interactions, such as host-parasite interactions [4].

Similarly, widespread cooperative plant-animal interactions are also important drivers of diversification. About 90% of flowering plants rely on animal pollinators to transfer their pollen [5], and about 90% of tropical plants rely on frugivorous animals to disperse their seeds [6]. Macroevolutionary studies from both phylogenetic and paleobiology perspectives support that these widespread cooperative interactions increased the diversification rate in both plants and animals [7–10].

But how cooperative interactions influence diversification is still unclear. In cooperative interactions, each partner improves the other's fitness, so both partners benefit from a

stable relationship. Previous work [11] suggests that in order to maximize its fitness, each partner in cooperative interactions needs to complement the phenotype of the other; *e.g.*, the timing of flowering of a plant matches with the eclosion timing of its insect pollinator. Any deviation from the phenotype matching will cause failure in the interaction and lower the fitness of both partners; thus, the phenotypes of both partners should be fixed by stabilizing selection (Box 1c). Consequently, cooperative interactions should hinder, rather than promote, diversification [11,12]. Although this obvious paradox between empirical observation of rapid diversification and theoretical expectation of phenotypic stasis has been recognized, a satisfactory mechanistic explanation for diversification mediated by cooperation is still lacking.

To address this paradox, I propose an alternative framework to understand cooperative interactions. Natural selection acts on each individual participant in any biological interaction, instead of on the partnership as a unit. Each party in the cooperative interaction is under selection to maximize its own fitness, which may or may not align with the other partner's fitness. Although each partner has a net fitness gain from engaging in a cooperative interaction, inherent conflicts of interest can still be present, thus influencing diversification in a manner similar to antagonistic interactions (Box 1b and 1d). Therefore, I suggest that, similar to antagonistic interactions, conflicts of interest in cooperative interactions are ubiquitous and could be the driving force promoting evolutionary diversification. This new framework – hidden conflicts of interest in seemingly cooperative interactions – can reconcile the paradox between previous theoretical understandings and empirical phylogenetic pattern of diversification in cooperative interactions.

Conflict of interest drives rapid diversification in antagonistic interactions
Rapid diversification happens frequently in species that engage in antagonistic interactions, such as predator-prey and host-parasite. Here, I provide a very brief summary of this topic, which is reviewed elsewhere [4,11–14].

The conflict of interest in antagonistic interactions imposes a fitness cost on one of the partners when the phenotypic difference is fixed; *e.g.,* phenotypic matching between the eggs of cuckoos and their hosts. Phenotypic diversification is likely to occur due to this fitness cost [11]. The phenotypic divergence within a species can lead to species diversification, especially when traits responsible for the conflict also influence reproductive isolation [14]; *e.g.,* if the diverging traits promote assortative mating.

Ample empirical evidence from both observations in nature and laboratory experiments validates that the conflict of interest in antagonistic interactions can lead to diversification. For example, in a predator-prey interaction, a snake (predator) with dietary specialization on snails and slugs evolved asymmetry in mandibular tooth number to easily grasp and eat snails (prey) with dextrally-coiled shells. Dextral snail populations adapted to the predation pressure with a reversal from dextrality to sinistrality. This adaptation also causes instant speciation in snails because of the mating difficulty between dextral and sinistral snails [15]. Similarly, the evolutionary arms race between lodgepole pine (prey) and its seed predator red crossbill leads to divergence in the lodgepole pine's cone structure, selecting for a corresponding counteradaptation in the bird's bill size. As a result, different red crossbill bill size morphs utilizing different food resources diverge in habitat use, occurrence of breeding, and call types, which together account for the nearly complete reproductive isolation among sympatric crossbill morphotypes [16]. Although a direct empirical test of the hypothesis that antagonistic coevolution drives diversification in the field is usually difficult because of the long time periods required, experimental evolution in microbial systems consistently supports the notion. For example, in several bacterium (host)-phage (pathogen) coevolution experiments, rapid genomic and phenotypic divergence in both bacterium and phage were observed [17,18].

Conflict of interest is ubiquitous in cooperative interactions

Conflicts of interest between cooperative partners are not as obvious as in antagonistic interactions; they nevertheless exist ubiquitously [19]. Theoretically, cooperation can only evolve if a participant's benefit:cost ratio of a mutualistic act is greater than a

threshold value [20]. Therefore, all cooperative interactions have both selfish components and mutualistic components. The mutualistic components of cooperation are usually more obvious, since cooperative interactions often are first identified based upon the observation of mutualistic acts. However, the selfish components of cooperation could still be manifested in a few different ways, such as the emergence of cheaters in a cooperating community (*e.g.*, some workers of eusocial insects lay their own eggs in the colony instead of tending the queen's eggs [21]), the occasional cheating behavior of a cooperating individual (*e.g.*, a hummingbird's "nectar robbing" behavior in lieu of pollination [22]), or the selfish nature of a cooperative act (*e.g.*, sexual cannibalism, such as female spider consuming her mate after copulation [23]). Below, I discuss conflicts of interest in some classical examples of cooperative interactions.

Sexual reproduction is an obvious intraspecific cooperative interaction because each sex needs the other to generate offspring. Despite the reciprocally beneficial nature of sexual reproduction, differences in optimal fitness strategies, such as mating frequency, lead to a strong conflict of interest between the two sexes [24]. A good example is seminal fluid influence on female *Drosophila*. Male *Drosophila* produce accessory gland proteins in their seminal fluid that induce female flies to increase egg-laying and reduce receptivity to future mating [25], which aligns with the interests of the male. However, these proteins also shorten the female *Drosophila*'s lifespan, thus reducing the female's fitness [26]. Female *Drosophila* respond with rapid evolution in the receptors targeted by male seminal fluid proteins, as a defense mechanism [27]. The evolutionary arms race between the sexes causes genes controlling sexual reproduction functions to evolve much faster than other genes [28]. Correspondingly, the traits involved in sexual signaling [29] and genitalia [30] also evolve and diverge more rapidly than other body traits.

In plant-pollinator interactions, plants provide resources (*e.g.*, nectar, habitat) to pollinators in exchange for the pollen transfer services that pollinators provide. One form of conflict in pollination is the amount of reward that plants invest in pollination. As the most common form of reward, nectar is costly for plants to produce (up to 37% of the plant's available energy). This costly nectar production reduces the amount of seeds that

the plant can produce [31]. While pollinators prefer a large nectar reward to maximize their benefit from the flowers they visit, plants prefer a small reward to reduce the cost. The partners have a conflict of interest over the optimal amount of nectar deployed in every flower [32]. Many orchid species produce flowers without nectar as Batesian mimics to sympatric nectar-producing model species, exploiting the pollinators' familiarity with the model species [33]. Because pollinators usually cannot detect the presence or absence of nectar until they enter the flower, the nectarless orchids receive pollination service while not paying the costly nectar reward to pollinators.

Brood pollination, such as fig and fig wasp and yucca and yucca moth, is a type of highly specialized cooperative interaction. In brood pollination, the insects are usually the exclusive pollinator species for the plants. But they also lay their eggs exclusively in female flowers, where the larvae consume plant tissues that would otherwise become seeds. There is a conflict of interest in producing viable seeds *vs*. insect larvae [34].

Cleaning symbiosis is another classical cooperative interaction, in which the cleaner eats the ectoparasites for its client, so the cleaner get its food while the client receives a health benefit. However, in fish cleaning symbioses, the cleaner fish also eats the mucus of the client fish, which they prefer over ectoparasites [35]. There is a conflict of interest between the two partners in the proportion of ectoparasites *vs*. mucus that the cleaner fish eats. The client responds to the cleaner fish's cheating behavior with predation on cleaner fish, or image scoring when the cleaner fish is working with other clients [36].

Besides these examples, conflict of interests have also been reported in a range of cooperative interactions, such as centromere drive in chromosome separation [37], quorum-sensing in bacteria [38], and between fungi and fungus-growing leafcutter ants [39]. In some cases, the conflicts of interest between interacting partners are so strong that the boundary between cooperative and antagonistic interaction becomes blurry. For example, a previously-described mutualistic cleaning symbiosis between oxpeckers and African ungulates turned out to be more parasitic than mutualistic, because oxpeckers

prefer to feed on blood from the ungulates' wounds rather than on the ungulates' tick parasites. Ungulates cannot effectively deter oxpecker's wound-feeding behavior [40,41]. Likewise, in a plant-pollinator interaction when the pollinator also oviposits in the flower, the interaction could be cooperative in some habitats but antagonistic in neighboring habitats, depending on the availability of co-pollinators [42].

As a result, the ubiquitous existence of conflict of interest suggest that cooperative interactions are better analyzed in a framework of "reciprocal exploitations that nonetheless provide net benefits to each partner" [19]. Antagonistic interactions and cooperative interactions are better viewed as the two ends of a continuous spectrum, instead of two qualitatively distinct categories. Incorporating this framework into studies of cooperative interactions can enhance our understanding of how cooperative interactions influence diversification (Box 1).

Conflict in cooperative interactions can promote diversification
The conflict of interest between cooperatively interacting partners can be conceptualized as different phenotypic optima in a fitness landscape (Box 1d). For example, in a plant-pollinator species pair, the optimal nectar volume for the pollinator is different from the plant. The differences in fitness optima will create diverging selective forces acting on both of the cooperating partners, disrupting a stable equilibrium of phenotype distributions and increasing the amount of phenotypic variation within each population. The increased phenotypic variation could be further promoted by genetic drift, geographic isolation, or assortative mating, and lead to population level phenotypic divergence.

Consistent with the predictions of the geographic mosaic theory of coevolution [43], the reciprocal divergent selection between cooperating partners can increase trait variation and create geographic mosaic patterns in the traits that strongly affect each partner's fitness. For example, an orchid and its pollinator have different fitness optima in the evolution of proboscis length and flower nectar spur length. The longer the pollinator's proboscis, the more efficiently it can get nectar from the flower, but its body is kept

further away from the flower, making it less likely to transfer the orchid's pollinia. The inverse effect happens when orchid evolves longer nectar spur. Both the pollinator's proboscis length and the orchid's nectar spur length are highly variable even at fine geographic scale, and their lengths usually match with each other in the same area [44,45]. Theoretical modeling and simulation support that the reciprocal selection generated by conflicts of interest between the orchid and its pollinator can promote population phenotypic divergence and create the observed geographic mosaic patterns [46]. Interestingly, a similar high level of trait variation and geographic covariation were reported in key traits that mediate antagonistic interactions; *e.g.,* the tetrodotoxin toxicity level of newts (prey) and the tetrodotoxin resistance level of garter snakes (predator) [47], the fruit coat thickness of Japanese camellia (prey) and the mouthpart length of the camellia weevil (seed predator) [48], and the virulence of the hymenopterous parasitoids (parasite) and the resistance of *Drosophila* larvae (host) [49].
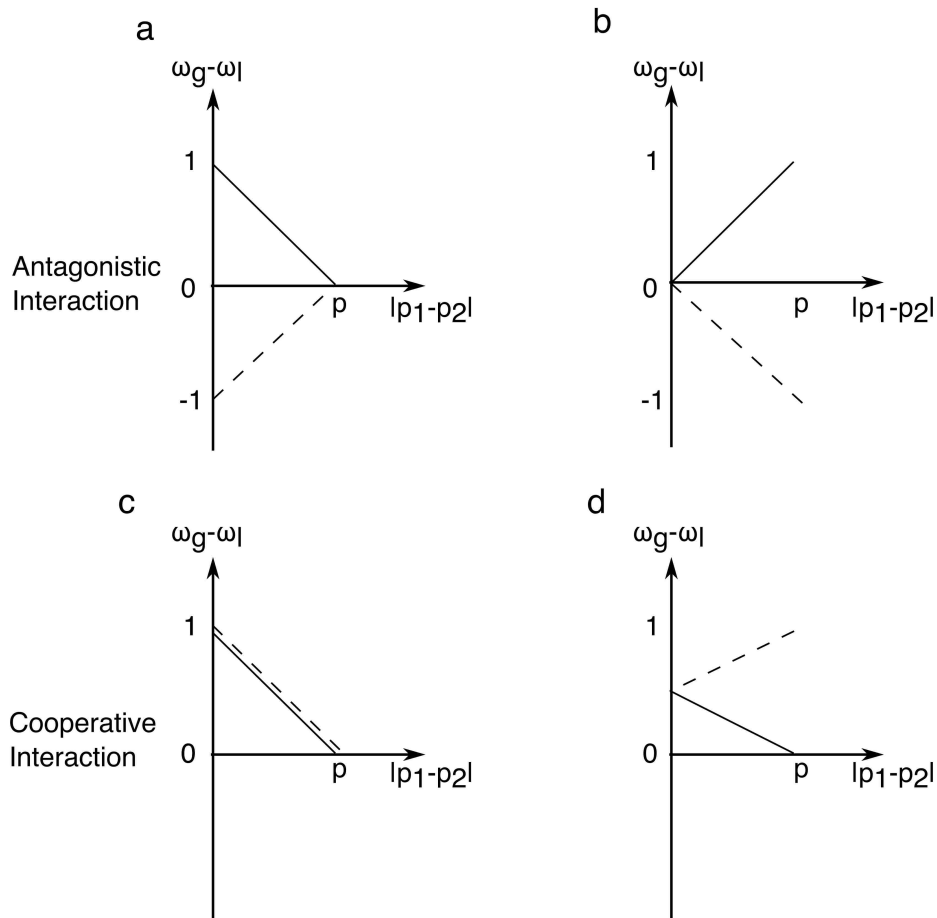
Phenotypic divergence is a function of time and the strength of selection. Several mechanisms can lead from phenotypic divergence to speciation. First, if there is geographic isolation among the diverging populations, post-zygotic isolation can arise by the evolution of Dobzhansky-Muller incompatibilities [50]. Such incompatibilities arise more quickly as a result of natural selection than by genetic drift alone. Second, some diverged populations may establish cooperative interactions with a new partner species, if the new partner can engage in a more successful interaction than the old partner. Further divergence and speciation could occur as a result of new adaptations to the new partner. For example, if a new pollinator guild can more efficiently feed on and pollinate a divergent plant population, the plant population might adapt and shift to the new pollinator guild. Pre-zygotic reproductive barriers could form as a result of the assortative mating mediated by the old and new pollinator guilds [51]. Lastly, a speciation event can also occur if the phenotypic divergence is directly associated with reproductive isolation. For example, in brood pollination, because the female insect's ovipositor is used both for egg-laying and mating, the diverging evolution of female insect's ovipositor length due to the conflict between host plant and insect could lead to corresponding divergence in male

insect reproductive structures, thus producing reproductive isolation from the original insect population [52].

Concluding remarks

To uncover the harmony and conflict between interacting partners is key to understanding how cooperative interactions could arise and drive diversification. Because natural selection acts on individual partners in biological interactions, instead of on the partnership as a unit, conflict of interest is ubiquitous in cooperative interactions. Most previous work on cooperative interactions overlooks this fact and focuses mostly on the mutually beneficial aspect, which leads to the conclusion that cooperative interactions hinder diversification. However, after surveying the studies on conflicts in cooperative interactions, I find that cooperative interactions and antagonistic interaction should better be viewed as two ends of a continuous spectrum, instead of two distinct categories. This unified coevolution framework suggests that the conflict of interest in cooperative interactions can also promote diversification, in a manner similar to antagonistic interactions.

Rapid diversification was reported in many cooperative systems [53–55], but the mechanisms of diversification are largely unknown. A promising future direction to understand how cooperative interactions affect diversification in those systems is to quantify the fitness effects of key traits that mediate cooperative interactions and to understand how the relative benefit *vs.* cost that the interaction incurs to the partners.

a

$\omega_g - \omega_l$

1

Antagonistic
Interaction 0   p |p₁-p₂|

-1

b

$\omega_g - \omega_l$

1

0   p |p₁-p₂|

-1

c

$\omega_g - \omega_l$

1

Cooperative
Interaction 0   p |p₁-p₂|

d

$\omega_g - \omega_l$

1

0   p |p₁-p₂|

Box 1

This diagram shows the different fitness effects of different types of antagonistic and cooperative interactions. The horizontal axis represents the absolute differences of the key trait pair that mediates interactions between two partners; *e.g.,* the difference in length between floral nectar tube and pollinator proboscis, the difference in appearance between mimic and model, or the difference in speed between predator and prey. For simplicity, I only consider two conditions: 0 represents perfectly matching phenotypes, while p represents unmatched phenotypes. The vertical axis represents the net fitness gain that each partner has from the interaction; *e.g.,* in a plant-pollinator interaction, for the plant it is the number of seeds fertilized by pollinator minus the energy cost to produce nectar, and for pollinator it is the energy gain from the nectar minus the energy

consumption for visiting the flower. Here, 0 represents 0 net fitness gain from the interaction, so it is equivalent to a free-living life style without interacting with the other partner. For antagonistic interactions, one partner has positive net fitness gain, while the other has negative net fitness gain. For cooperative interactions, both partners have positive net fitness gain.

(a) Phenotype-matching antagonistic interaction. For example, in brood parasitism, when the appearance of the brood parasite's egg (solid line) perfectly matches the host's eggs (dashed line) ($|p_1-p_2| = 0$), the parasite has the largest positive net fitness gain while the host has the largest negative net fitness gain. (b) Phenotype-differing antagonistic interaction. For example, in a predator-prey interaction, the predator (solid line) has the highest positive net fitness gain when its speed exceeds that of the prey (dashed line) ($|p_1-p_2| = p$). (c) Cooperative interaction when there is no conflict of interest. For example, when the timing of flowering matches with the timing of the insect pollinator's eclosion ($|p_1-p_2| = 0$), both partners have the largest positive net fitness gain. (d) Cooperative interaction when there is a conflict of interest. For example, in orchid pollination, a longer nectar spur will bring the plant (dashed line) its highest net fitness gain ($|p_1-p_2| = p$), but the pollinator's (solid line) can barely get nectar, reducing its net fitness gain below the maximum value.

Outstanding Questions

What are the hidden conflicts in other cooperative systems? The traits that mediate interaction and strongly affect each partner's fitness (*e.g.,* plant's nectar volume in plant-pollinator interaction) and the traits that evolve more rapidly than average (*e.g.,* genitalia) are good candidates to study.

How do conflicts of interest in cooperative systems promote initial phenotypic divergence at the microevolutionary scale? Microbial coevolution experiments can provide the most direct test of the hypothesis that conflicts of interest promote diversification, but most previous coevolution experiments only focused on antagonistic interactions.

What are the respective roles that conflicts of interest and other isolating mechanisms, such as geographic isolation, play in promoting diversification? Are conflicts of interest necessary and sufficient in explaining speciation of cooperative partners?

How does the level of specialization of species interaction influence the outcome of the conflicts of interest? Strong conflicts in generalized cooperative interactions could lead to cooperation breakdown and reformation with other partners, but this option is limited for specialized interaction. Different mode of cooperative interaction could have different impacts on diversification.

What are the similarities between antagonistic and cooperative interactions in promoting diversification? Most previous theoretical works treats them as two categorically different interactions and model them separately. But it is clear that in some cases the distinction is not clear-cut. Thus a unified framework is useful in understanding the general characteristics of coevolutionary diversification.

Acknowledgement

References

1   Friedman, W.E. (2009) The meaning of Darwin's "abominable mystery". *Am. J. Bot.* 96, 5–21

2   Ehrlich, P.R. and Raven, P.H. (1964) Butterflies and Plants: A Study in Coevolution. *Evolution* 18, 586

3   Bascompte, J. and Jordano, P. (2007) Plant-Animal Mutualistic Networks: The Architecture of Biodiversity. *Annu. Rev. Ecol. Evol. Syst.* 38, 567–593

4   Summers, K. *et al.* (2003) Parasitic exploitation as an engine of diversity. *Biol. Rev. Camb. Philos. Soc.* 78, 639–675

5   Ollerton, J. *et al.* (2011) How many flowering plants are pollinated by animals? *Oikos* 120, 321–326

6   Jordano, P. and others (2000) Fruits and frugivory. *Seeds Ecol. Regen. Plant Communities* 2, 125–166

7   Dodd, M.E. *et al.* (1999) Phylogenetic analysis of trait evolution and species diversity variation among angiosperm families. *Evolution* 53, 732–744

8   Grimaldi, D. (1999) The co-radiations of pollinating insects and angiosperms in the Cretaceous. *Ann. Mo. Bot. Gard.* 86, 373–406

9   Gómez, J.M. and Verdú, M. (2012) Mutualism with Plants Drives Primate Diversification. *Syst. Biol.* 61, 567–577

10   Rojas, D. *et al.* (2012) The role of frugivory in the diversification of bats in the Neotropics. *J. Biogeogr.* 39, 1948–1960

11   Yoder, J.B. and Nuismer, S.L. (2010) When does coevolution promote diversification? *Am. Nat.* 176, 802–817

12   Hembry, D.H. *et al.* (2014) Coevolution and the Diversification of Life. *Am. Nat.* 184, 425–438

13   Brockhurst, M.A. and Koskella, B. (2013) Experimental coevolution of species interactions. *Trends Ecol. Evol.* 28, 367–375

14   Althoff, D.M. *et al.* (2014) Testing for coevolutionary diversification: linking pattern with process. *Trends Ecol. Evol.* 29, 82–89

15   Hoso, M. *et al.* (2010) A speciation gene for left-right reversal in snails results in anti-predator adaptation. *Nat. Commun.* 1, 133

16   Smith, J.W. and Benkman, C.W. (2007) A Coevolutionary Arms Race Causes Ecological Speciation in Crossbills. *Am. Nat.* 169, 455–465

17   Paterson, S. *et al.* (2010) Antagonistic coevolution accelerates molecular evolution. *Nature* 464, 275–U154

18   Marston, M.F. *et al.* (2012) Rapid diversification of coevolving marine Synechococcus and a virus. *Proc. Natl. Acad. Sci.* 109, 4544–4549

19   Herre, null *et al.* (1999) The evolution of mutualisms: exploring the paths between conflict and cooperation. *Trends Ecol. Evol.* 14, 49–53

20   Nowak, M.A. (2006) Five Rules for the Evolution of Cooperation. *Science* 314, 1560–1563

21   Beekman, M. and Oldroyd, B.P. (2008) When Workers Disunite: Intraspecific Parasitism by Eusocial Bees. *Annu. Rev. Entomol.* 53, 19–37

22   Irwin, R.E. *et al.* (2010) Nectar Robbing: Ecological and Evolutionary Perspectives. *Annu. Rev. Ecol. Evol. Syst.* 41, 271–292

23   Elgar, M.A. and Schneider, J.M. (2004) Evolutionary significance of sexual cannibalism. *Adv. Study Behav.* 34, 135–163

24   Chapman, T. *et al.* (2003) Sexual conflict. *Trends Ecol. Evol.* 18, 41–47

25   Ravi Ram, K. and Wolfner, M.F. (2007) Seminal influences: Drosophila Acps and the molecular interplay between males and females during reproduction. *Integr. Comp. Biol.* 47, 427–445

26   Chapman, T. *et al.* (1995) Cost of mating in Drosophila melanogaster females is mediated by male accessory gland products. *Nature* 373, 241–244

27   Rice, W.R. (2000) Dangerous liaisons. *Proc. Natl. Acad. Sci.* 97, 12953–12955

28   Swanson, W.J. and Vacquier, V.D. (2002) The rapid evolution of reproductive proteins. *Nat. Rev. Genet.* 3, 137–144

29   Yeh, P.J. and Benkman, C. (2004) Rapid evolution of a sexually selected trait following population establishment in a novel habitat. *Evolution* 58, 166–174

30   Hosken, D.J. and Stockley, P. (2004) Sexual selection and genital evolution. *Trends Ecol. Evol.* 19, 87–93

31   Pyke, G.H. (1991) What does it cost a plant to produce floral nectar? *Nature* 350, 58–59

32   Bronstein, J.L. (2001) The exploitation of mutualisms. *Ecol. Lett.* 4, 277–287

33   Johnson, S. (2000) Batesian mimicry in the non-rewarding orchid Disa pulchra, and its consequences for pollinator behaviour. *Biol. J. Linn. Soc.* 71, 119–132

34   Herre, E.A. and West, S.A. (1997) Conflict of interest in a mutualism: documenting the elusive fig wasp–seed trade–off. *Proc. R. Soc. Lond. B Biol. Sci.* 264, 1501–1507

35   Grutter, A.S. and Bshary, R. (2003) Cleaner wrasse prefer client mucus: support for partner control mechanisms in cleaning interactions. *Proc. R. Soc. Lond. B Biol. Sci.* 270, S242–S244

36   Bshary, R. and Grutter, A.S. (2006) Image scoring and cooperation in a cleaner fish mutualism. *Nature* 441, 975–978

37   Malik, H.S. (2009) The centromere-drive hypothesis: a simple basis for centromere complexity. In *Centromere* pp. 33–52, Springer

38   Diggle, S.P. *et al.* (2007) Cooperation and conflict in quorum-sensing bacterial populations. *Nature* 450, 411–414

39   Mueller, U.G. (2002) Ant versus Fungus versus Mutualism: Ant-Cultivar Conflict and the Deconstruction of the Attine Ant-Fungus Symbiosis. *Am. Nat.* 160, S67–S98

40   Weeks, null (1999) Interactions between red-billed oxpeckers, Buphagus erythrorhynchus, and domestic cattle, Bos taurus, in Zimbabwe. *Anim. Behav.* 58, 1253–1259

41   Plantan, T. *et al.* (2013) Feeding preferences of the red-billed oxpecker, Buphagus erythrorhynchus: a parasitic mutualist? *Afr. J. Ecol.* 51, 325–336

42   Thompson, J.N. and Cunningham, B.M. (2002) Geographic structure and dynamics of coevolutionary selection. *Nature* 417, 735–738

43   Thompson, J.N. (2005) *The geographic mosaic of coevolution*, University of Chicago Press.

44   Anderson, B. and Johnson, S.D. (2009) Geographical covariation and local convergence of flower depth in a guild of fly-pollinated plants. *New Phytol.* 182, 533–540

45   Pauw, A. *et al.* (2009) Flies and flowers in Darwin's race. *Evolution* 63, 268–279

46   Zhang Feng *et al.* (2013) Adaptive divergence in darwin's race: how coevolution can generate trait diversity in a pollination system. *Evolution* 67, 548–560

47   Brodie, E.D. *et al.* (2002) The Evolutionary Response of Predators to Dangerous Prey: Hotspots and Coldspots in the Geographic Mosaic of Coevolution Between Garter Snakes and Newts. *Evolution* 56, 2067–2082

48   Toju, H. and Sota, T. (2006) Imbalance of predator and prey armament: geographic clines in phenotypic interface and natural selection. *Am. Nat.* 167, 105–117

49   Kraaijeveld, A.R. and Godfray, H.C.J. (1999) Geographic Patterns in the Evolution of Resistance and Virulence in Drosophila and Its Parasitoids. *Am. Nat.* 153, S61–S74

50   Orr, H.A. and Turelli, M. (2001) The evolution of postzygotic isolation: accumulating dobzhansky-muller incompatibilities. *Evolution* 55, 1085–1094

51   Whittall, J.B. and Hodges, S.A. (2007) Pollinator shifts drive increasingly long nectar spurs in columbine flowers. *Nature* 447, 706–709

52   Althoff, D.M. (2014) Shift in Egg-Laying Strategy to Avoid Plant Defense Leads to Reproductive Isolation in Mutualistic and Cheating Yucca Moths. *Evolution* 68, 301–307

53   Janson, E.M. *et al.* (2008) Phytophagous insect–microbe mutualisms and adaptive evolutionary diversification. *Evolution* 62, 997–1012

54   Lengyel, S. *et al.* (2009) Ants Sow the Seeds of Global Diversification in Flowering Plants. *PLOS ONE* 4, e5480

55   Litsios, G. *et al.* (2012) Mutualism with sea anemones triggered the adaptive radiation of clownfishes. *BMC Evol. Biol.* 12, 212